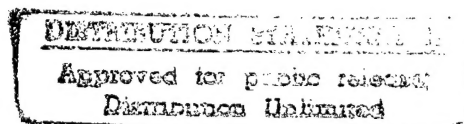# Theoretical Studies of the Dynamics of Condensed Phase High Energy Density Materials

Gregory A. Voth

Department of Chemistry
University of Pennsylvania
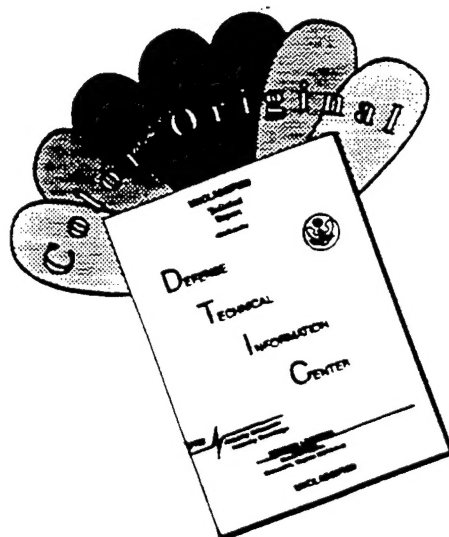Philadelphia PA 19104-6323

April 1997

Final Report

19970523 047

PHILLIPS LABORATORY
Propulsion Directorate
AIR FORCE MATERIEL COMMAND
EDWARDS AIR FORCE BASE CA 93524−7048

DISCLAIMER NOTICE

THIS DOCUMENT IS BEST QUALITY AVAILABLE. THE COPY FURNISHED TO DTIC CONTAINED A SIGNIFICANT NUMBER OF COLOR PAGES WHICH DO NOT REPRODUCE LEGIBLY ON BLACK AND WHITE MICROFICHE.
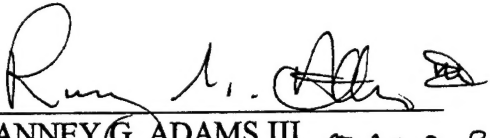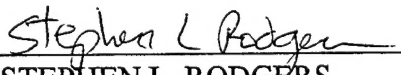
NOTICE

When U.S. Government drawings, specifications, or other data are used for any purpose other than a definitely related Government procurement operation, the fact that the Government may have formulated, furnished, or in any way supplied the said drawings, specifications, or other data, is not to be regarded by implication or otherwise, or in any way licensing the holder or any other person or corporation, or conveying any rights or permission to manufacture, use or sell any patented invention that may be related thereto.

FOREWORD

This final technical report, entitled *Theoretical Studies of the Dynamics of Condensed Phase High Energy Density Materials,* presents the results of a study performed by the University of Pennsylvania, Philadelphia, PA, under Contract No. F04611-91-K-0006. The Project Manager for Phillips Laboratory was Dr. Jerry A. Boatz.

JERRY A. BOATZ
Project Manager

RANNEY G. ADAMS III
Director,
Public Affairs

STEPHEN L. RODGERS
Director
Propulsion Sciences Division

REPORT DOCUMENTATION PAGE

1. AGENCY USE ONLY (LEAVE BLANK	2. REPORT DATE April 1997	3. REPORT TYPE AND DATES COVERED Final 01 Jan 91 – 30 Sep 96

4. TITLE AND SUBTITLE

Theoretical Studies of the Dynamics of Condensed Phase High Energy Density Materials

6. AUTHOR(S)

Gregory A. Voth

5. FUNDING NUMBERS

C: F04611-91-K-0006
PE: 62601F
PR: 3058
TA: 00CW

7. PERFORMING ORGANIZATION NAME(S) AND ADDRESS(ES)

Department of Chemistry
University of Pennsylvania
Philadelphia PA 19104-6323

8. PERFORMING ORGANIZATION REPORT NUMBER

9. SPONSORING/MONITORING AGENCY NAME(S) AND ADDRESS(ES)

Phillips Laboratory
OL-AC PL/RKS
10 East Saturn Blvd.
Edwards AFB CA 93524-7680

10. SPONSORING/MONITORING AGENCY REPORT NUMBER

PL-TR-96-3028

11. SUPPLEMENTARY NOTES

COSATI CODE(S): 2109; 210902; 2010

12a. DISTRIBUTION/AVAILABILITY STATEMENT

Approved for Public Release; Distribution Unlimited.

12b. DISTRIBUTION CODE

A

13. ABSTRACT (MAXIMUM 200 WORDS)

Quantum solids such as hydrogen, which contain matrix isolated reactive species such as atomic lithium, boron, hydrogen, nitrogen, organic radicals, etc., have been suggested as possible high energy density matter (HEDM) for propulsion purposes. At temperatures appropriate to the condensed phases of hydrogen, both the light guest species and the host solid molecules exhibit very significant quantum mechanical effects. This report describes the development and application of quantum mechanical methods to computationally probe the dynamical and structural behavior of impurity species (e.g., atomic lithium) in solid, liquid, and cluster *para*-hydrogen. These studies were based on the Feynman path integral formulation of statistical mechanics. Both the structural and dynamical aspects of the composite condensed phase systems are reported. The long-range strategic goal of the research program was to develop a computational methodology for predicting the stability of prospective cryogenic HEDM.

14. SUBJECT TERMS

high energy density matter; HEDM; quantum solid; computer simulation

15. NUMBER OF PAGES

45

16. PRICE CODE

.

17. SECURITY CLASSIFICATION OF REPORT	18. SECURITY CLASSIFICATION OF THIS PAGE	19. SECURITY CLASSIFICATION OF ABSTRACT	20. LIMITATION OF ABSTRACT
Unclassified	Unclassified	Unclassified	SAR

Standard Form 298 (Rev 2-89)
Prescribed by ANSI Std 239-18
298-102

TABLE OF CONTENTS

LIST OF FIGURES

GLOSSARY

AFOSR	Air Force Office of Scientific Research
a.u.	atomic units
B	boron
CGMP	centroid potential of mean force
CMD	Centroid Molecular Dynamics
D	diffusion constant
D_2	molecular deuterium
DoD	Department of Defense
ESR	electron spin resonance
F	free energy
GB	Gibbs-Bogoliubov
GFLOPS	billion floating point operations per second
H	hydrogen
H_2	hydrogen gas
hcp	hexagonal close packed
HEDM	high energy density matter
HPCMD	Hyper-Parallel Centroid Molecular Dynamics
k	rate constant
Li	lithium
M	number of time steps
MC	Monte Carlo
MD	molecular dynamics
MFLOPS	million floating point operations per second
P	discretization parameter
PIMC	path integral Monte Carlo
PIMD	path integral Molecular Dynamics

r	position
T	temperature
TST	transition state theory
Z	quantum partition function

Greek

Φ	intermolecular pair potential
ψ	atomic wave function
ν	velocity

1.0 INTRODUCTION

1.1 Aims of the Research

Solid hydrogen doped with atomic impurities[1,2] (e.g., Li, B, H) is potential high energy density matter (HEDM) for use in rocket propulsion. One critical issue in these materials is the metastable structure of the impurity trapping sites. This issue was a primary focus of research in the HEDM Program over the past five years (see Sec. 2.0 Research Results, Data Obtained and Accomplishments). However, a second and probably even more important issue is the rate of diffusion and recombination of impurities in the solid hydrogen host. This second issue became the focus of the research in the final two years, and it is presently the focus of the Air Force Office of Scientific Research (AFOSR)-funded continuation of the project. Indeed, the ability to "scale-up" potential cryogenic HEDMs in order to achieve an impurity concentration of a few mole percent – and to have this material be stable for a reasonable period of time – is perhaps the central issue that must be addressed before such materials can be usefully employed in propulsion systems. Thus, the timescale for recombination of the energy-storing impurity species within the condensed phase host is the key physical parameter that characterizes the overall stability of the HEDM. Ideally, the timescale for the recombination reactions should be at least on the order of days, depending of course on the specific use of the material.

Theoretical studies can help us to understand the key features that govern the stability of a HEDM. For example, the average rate of impurity recombination in condensed matter is usually governed by two dynamical timescales: the rate of impurity self-diffusion and the intrinsic (i.e., local) rate of impurity recombination. The overall recombination process in low temperature solid HEDM may, therefore, be characterized as a diffusion-influenced chemical reaction having a rate constant k_r for the macroscopic recombination rate. This fundamentally important constant – which has become the target of the theoretical investigations – is approximately given by the equation[3-6]

$$\frac{1}{k_r} \approx \frac{1}{k_{in}} + \frac{1}{k_D} \tag{1}$$

where k_{in} is the intrinsic recombination rate for the two impurities (i.e., after reaching some "contact" distance r_c) and k_D is the rate at which the two impurities diffuse into proximity with one another. The latter rate is related to the impurity self-diffusion constant D such that $k_D \approx 4\pi r_c D$. As may be readily verified by inspection of Equation 1, the impurity self-diffusion process limits the rate when $k_D \ll k_{in}$, whereas the microscopic recombination step is rate limiting if $k_{in} \ll k_D$.

Both the self-diffusion and recombination dynamics of atomic impurities in solid matrices involve complicated dynamical processes. In such processes, a particle may need to surmount (or tunnel through) a barrier in the effective potential energy surface along some "reaction coordinate" in order to reach a new stable/metastable state.[7-13] For the diffusion process, the guest atom may

move in a series of uncorrelated hops between the potential energy minima in the condensed phase host, or it may follow a mobile vacancy. In the recombination step, the diffusing atom may undergo an activated transition[14] to occupy the same site as a second guest atom, allowing a bond to be formed with that atom. The latter process would be quite exothermic in a cryogenic HEDM. The interaction of the diffusing particle with the condensed phase matrix provides an overall macroscopic free energy barrier to recombination, thereby leading to a metastable material.

Based on the above picture, it became apparent that a better microscopic understanding of both the impurity diffusion and recombination rates in low temperature HEDM was (and still is) necessary in order to characterize their stability. The present contract was the first condensed matter theoretical project funded by the Air Force to study the behavior of cryogenic HEDMs when this problem became a research priority in the early 1990s. Expertise in condensed matter theory and simulation was brought to bear on the problem, as well as expertise in high performance computing, which proved to be an asset to the HEDM Program. During the period of the contract, the focus was to develop and apply both quantum path integral simulation and analytical methods, with the early goal being the modeling of the trapping sites and spectroscopy of reactive impurity species such as lithium or hydrogen atoms in the solid para-hydrogen matrix. These efforts were in no small part motivated by the experimental work of Fajardo[1,2] and co-workers at Phillips Laboratory at Edwards AFB. The computational studies in the second part of the project were then aimed at understanding the microscopic factors that directly influence the fundamental dynamical process of impurity diffusion and recombination. These studies required a novel theoretical/ computational methodology to carry them out, as explained in the next paragraph.

The cryogenic HEDM systems based on solid hydrogen (e.g., Li in H_2) involve atomic impurities embedded in a low temperature solid hydrogen matrix.[15,16] Under normal conditions hydrogen solidifies around 14 K. Solid state theories usually contained in textbooks are inadequate to describe the physical properties (e.g., vibrational excitations) of this "quantum solid." About 20 years ago, solid hydrogen was widely studied precisely because the large zero–point anharmonic vibrational motion of the lattice molecules imbued this system with interesting properties. These quantum mechanical effects are extremely difficult to treat from the point of view of dynamical computer simulation. Why is this? Consider the case of the impurity self-diffusion. The diffusion constant can be obtain from either of two formulas:

$$D = \frac{1}{6} \lim_{t \to \infty} \frac{d}{dt} \langle |\mathbf{q}(t) - \mathbf{q}(0)|^2 \rangle \tag{2}$$

or

$$D = \frac{1}{3} \int_0^\infty dt \langle \dot{\mathbf{q}}(t) \cdot \dot{\mathbf{q}}(0) \rangle \tag{3}$$

where the notation $A(t) \equiv e^{iHt/\hbar} A e^{-iHt/\hbar}$ denotes a quantum Heisenberg operator for any operator "A". Both of the above functions are many-body quantum dynamical correlation functions [or, in

2

the case of Equation 2, can simply be related to one]. Similarly, the intrinsic dynamical recombination step of two impurities can be described by "product state" population correlation functions.

In a quantum solid such as hydrogen, the above quantum time correlation functions cannot be approximated using the classical Newtonian molecular dynamics (MD) method. The centerpiece of the final two years of the project, therefore, became the development and application of a new method developed by Cao and Voth[17-20] for computing quantum dynamical time correlation functions such as those above. In fact, it is the strength of this method, called Centroid Molecular Dynamics (CMD), which, for the first time, made it possible to study the quantum dynamics of quantum solids, with and without impurities. This method is now making it possible to study the self-diffusion and recombination processes of impurities in cryogenic HEDM via computer simulation and, thereby, to probe the microscopic origins of HEDM instabilities.

This research project has been both critical and timely for the Air Force HEDM Program. As the HEDM program moves into the future, the methodology developed during the Air Force contract can be expected to play an important role in determining the feasibility of "scaling-up" certain target materials. With the various Department of Defense (DoD) High Performance Computing Centers becoming increasingly functional, the methods developed with the support of this contract are being implemented on extraordinarily powerful parallel computing platforms. This should, in turn, lead to condensed phase HEDM simulations of an unprecedented scale and scope, while addressing some very challenging problems in condensed matter theory.

1.2 Brief Summary of the Research Results

• The most important result obtained during the contract period was the first calculation of the quantum mechanical barrier to recombination of two atomic lithium impurities in solid hydrogen at 4 K. The barrier was found to be on the order of 130 K, raising the theoretical possibility of trapping lithium impurities in solid hydrogen at concentrations of over 1 mol percent. Though preliminary, this is the first result of its kind and is encouraging for the low temperature solid hydrogen fuel effort of the Air Force HEDM Program.

• A computational approach to study low temperature HEDM was developed called CMD, which incorporates the dominant quantum dynamical effects of a many-body system into a classical MD framework. A powerful CMD algorithm was also developed called Hyper-Parallel CMD (HPCMD), which recently achieved 3.1 billion floating point operations per second (GFLOPS) performance with 80% computational efficiency over 64 nodes on the DoD Maui High Performance Computing Center IBM SP2.[21]

3

• As a test of the CMD methodology, the quantum self-diffusion constant for liquid para-hydrogen was computed for several temperatures and successfully compared by experiment. These simulations demonstrated both the accuracy of the method and scalability of the CMD algorithm.[22]

• The quantum phonon spectrum for para-hydrogen at 4 K was also computed and successfully compared by experiment. These results demonstrated the ability to reliably study low temperature hydrogen systems of interest to the Air Force HEDM Program through largescale parallel CMD simulations.

• Two analytical models for atomic impurities in solid hydrogen were developed, which have been used to predict the equilibrium structure and thermodynamic properties of such HEDMs.[23,24]

• The nature of the impurity sites for lithium atoms in solid para-H_2 and ortho-D_2 were determined with quantum computer simulation methods. The electronic excitation spectrum was also calculated and found to agree well with the experimental spectrum that Fajardo and co-workers obtained at PL, Edwards.[25]

• The electron spin resonance (ESR) linewidth for a hydrogen atom impurity in solid p-H_2 was calculated from first principles and found to be in agreement with the CMD experiment. The linewidth was predicted to be the same for substitutional and interstitial impurity sites in the lattice. This study suggested that H-atom impurities in solid hydrogen are likely to be quite mobile and, thus, may not be a good HEDM candidate.[26]

• The behavior of a Li atom in liquid and cluster p-H_2 was studied through quantum computer simulation methods.[27]

• The behavior of clusters of p-H_2 were studied by quantum computer simulation methods.[28-30]

2.0 RESEARCH RESULTS, DATA OBTAINED, AND ACCOMPLISHMENTS

2.1 Advances in Theoretical Methodology

Richard Feynman demonstrated that quantum statistical mechanics could be reformulated in terms of path integrals.[31,32] For example, the partition function for a system is given by the expression

4

$$Z = \int \cdots \int D\mathbf{q}(\tau)\, exp\{-S[\mathbf{q}(\tau)]/\hbar\} \tag{4}$$

where the functional integration is over all possible paths of the particles $\mathbf{q}(\tau)$, and $S[\mathbf{q}(\tau)]$ is the imaginary time action functional, given by

$$S[\mathbf{q}(\tau)] = \int_0^{\hbar\beta} d\tau \left\{ \frac{1}{2}\dot{\mathbf{q}}^\dagger(\tau) \cdot \mathbf{m} \cdot \dot{\mathbf{q}}(\tau) + V[\mathbf{q}(\tau)] \right\} \tag{5}$$

While the numerical evaluation of the equilibrium properties of a condensed phase system using Equation 4 might seem rather daunting, such calculations can actually be readily performed.[33-38] The simplest approach involves the "primitive" discretization of the path integral for the partition function into P "imaginary time slices," giving a formula valid for sufficiently large values of P, i.e.,

$$Z = \lim_{P \to \infty} \prod_{j=1}^{N} (m_j / 2\pi\hbar^2\varepsilon)^{3P/2} \int \cdots \int d\mathbf{q}_1 \cdots d\mathbf{q}_P \, exp\left[-\beta V_{eff}(\mathbf{q}_1,...,\mathbf{q}_P)\right] \tag{6}$$

where ε equals β / P and the isomorphic effective classical potential is given by

$$V_{eff}(\mathbf{q}_1,...,\mathbf{q}_P) = \sum_{i=1}^{P} \left[\frac{mP}{2\hbar^2\beta^2}(\mathbf{q}_i - \mathbf{q}_{i+1})^2 + \frac{1}{P}V(\mathbf{q}_i) \right] \tag{7}$$

and the subscript "i" denotes the coordinate of the particle at imaginary time $\tau = (i-1)\hbar\varepsilon$. For the calculation of properties using the partition function, the discretized paths are cyclic so that $\mathbf{q}_i$ equals $\mathbf{q}_{P+i}$. The primitive discrete representation of the path integral is isomorphic, with a classical partition function for a polymer composed of particles located at the positions $\{\mathbf{q}_i\}$ (Fig. 1). As can be deduced from Equations 6 and 7, the equilibrium properties of condensed matter systems having general potentials can be readily evaluated on a computer by Metropolis Monte Carlo (MC) techniques.[39] Many studies have now appeared in the literature in which path integral Monte Carlo (PIMC) or path integral Molecular Dynamics (PIMD) have been employed to simulate a quantum particle (or particles) in very complex environments involving hundreds or even thousands of atoms and/or molecules.[33-38] Interestingly, there had been only one other path integral simulation of solid hydrogen[40] before those carried out under the present contract. Moreover, the latter simulations were the only ones to study impurities in solid hydrogen. Indeed, it is largely the strength of this path integral simulation approach for complicated many-body systems that allowed the first direct calculations of a Li atom trapped in a solid p–H_2 matrix.
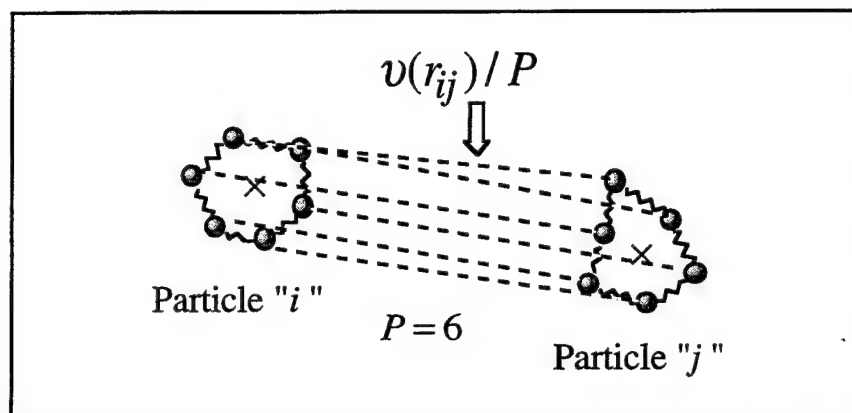
Figure 1
A Schematic of Two Quantum Particles Interacting Through a
Pairwise Potential in the Discretized Path Integral Representation

In Figure 1, each quantum particle is represented by an isomorphic classical-like "polymer" of P quasiparticles having harmonic intrapolymer interactions and pairwise interpolymer interactions. The value of the discretization parameter P in this case is 6, while a value of 50-100 is typically used to represent each quantum p–H_2 molecule in the spherical ($J = 0$) approximation at a temperature of 3-5 K.

Whereas the research supported by the contract over the first three years was focused on the structure of the trapping sites for impurities in solid hydrogen, research in the last two years began to directly address the dynamical problem of impurity diffusion and recombination in low temperature HEDMs. The basic components of this problem were outlined in Section 1.1 (Aims of Research). If such dynamical studies were to be carried out, however, they would need to be quantum dynamical studies [i.e., involving the effect of the quantum time evolution operator $\exp(-iHt/\hbar)$]. For low temperature HEDM systems, this represented an insurmountable challenge, since to solve the time-dependent Schrödinger equation for a low-temperature, nonlinear many-body system was essentially impossible (at least exponentially difficult!). Fortunately, a key theoretical breakthrough allowed study through computer simulation of the quantum dynamics of low temperature solids, and is now leading to direct studies of impurity diffusion and recombination in cryogenic HEDM. This breakthrough is called Centroid Molecular Dynamics.[17-20]

In "standard" equilibrium path integral simulations,[33-38] the isomorphic quasiparticle polymer (Fig. 1) representing a quantum particle is spread out in space, but it collapses towards a point particle and becomes more classical-like in the limit of high temperature or large mass. It seems reasonable, therefore, that the most classical-like variable for describing the equilibrium configurations of a quantum particle must be the path centroid variable,[17-20, 41-47] defined in the discretized path integral formalism by

$$\mathbf{q}_0 = \frac{1}{P}\sum_{i=1}^{P}\mathbf{q}_i \tag{8}$$

where $\mathbf{q}_i$ are the coordinates of the collection of P quasiparticles that represent the quantized physical particle [Equations 6 and 7]. In the continuous path picture, the centroid variable is given by

$$\mathbf{q}_0 = \lim_{P\to\infty}\frac{1}{P}\sum_{i=1}^{P}\mathbf{q}_i = \frac{1}{\hbar\beta}\int_0^{\hbar\beta}d\tau\,\mathbf{q}(\tau) \tag{9}$$

From the latter equation, it is easy to see that as $\hbar\beta \to 0$ (i.e., as $\hbar \to 0$ or $T \to \infty$) the Feynman paths that represent the delocalized quantum particle will shrink down to a classical point particle. However, when the system is fully quantized, the path centroid will be a "ghost" variable within the context of quantum Boltzmann statistical mechanics.

Before describing the results on the dynamical implications of the path centroid variable,[17-20] it is important to note that the interesting equilibrium properties of the centroid were first discovered and exploited by Feynman in his analysis of the quantum corrections to the classical partition function.[41-42] In that work, Feynman defined a path integral "centroid density," given by

$$\rho_c(\mathbf{q}_c) = \int\cdots\int D\mathbf{q}(\tau)\delta(\mathbf{q}_c - \mathbf{q}_0)\,exp\{-S[\mathbf{q}(\tau)]/\hbar\} \tag{10}$$

with the goal of deriving a simplified quasiclassical partition function. This equilibrium density is calculated by fixing the centroid variable in Equation 10 to a point in space $\mathbf{q}_c$ and then integrating over-all path fluctuations about the fixed centroid. In the discretized path integral picture, one instead integrates over-all configurations of the discretized quasiparticles having a fixed centroid, subject to the weighting by their effective Boltzmann-like configurational factor. In either case (continuous or discretized), the centroids of the Feynman paths are located at the position in space denoted by q_c. A kind of "centroid statistical mechanics" can then be defined based on the centroid potential $V_c(\mathbf{q}_c)$, defined from the path centroid density by

$$exp[-\beta V_c(\mathbf{q}_c)] = \int\cdots\int D\mathbf{q}(\tau)\delta(\mathbf{q}_c - \mathbf{q}_0)\,exp\{-S[\mathbf{q}(\tau)]/\hbar\} \tag{11}$$

where a normalization factor has been set to unity. The quantum partition function Z can be determined from Equation 11 by integrating over-all possible centroid positions (i.e., the centroid trace) such that

$$Z = \int d\mathbf{q}_c\rho_c(\mathbf{q}_c) = \int d\mathbf{q}_c\,e^{-\beta V_c(\mathbf{q}_c)} \tag{12}$$

Because of the nature of the path centroid variable, the centroid density in Equations 10 and 11 is the quantum equivalent to the classical Boltzmann density for the particle's equilibrium configurations.

While the centroid picture in equilibrium statistical mechanics is interesting in its own right, it was the discovery[17,18] and subsequent derivation[19] of the dynamical properties of the centroid

7

variable that have made research on impurity diffusion and recombination in low temperature solids possible. The basic result of CMD is that time correlation functions for quantum particles in many-body systems can be approximated by centroid time correlation functions obtained from running trajectories on the effective quantum centroid potential (cf. Fig. 2).
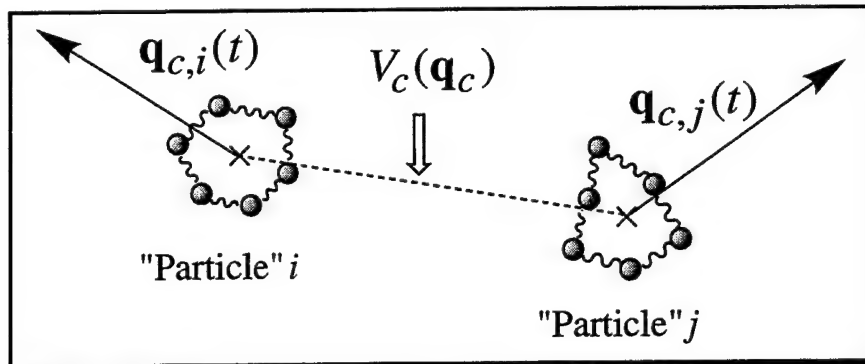
Figure 2
A Schematic of the Trajectories of Two Quantum Centroid "Particles"
Evolving in Time According to the CMD Equations

In Figure 2, the two centroid quasiparticles interact through the effective, temperature-dependent centroid potential.

The centroid trajectories $\mathbf{q}_c(t)$ in CMD are generated by the CMD equation

$$\mathbf{m} \cdot \ddot{\mathbf{q}}_c(t) = - \bar{\nabla}_c V_c(\mathbf{q}_c) \tag{13}$$

where $\mathbf{m}$ is the diagonal particle mass matrix and the effective centroid potential is defined according to Equation 11 as

$$V_c(\mathbf{q}_c) = - k_B T \ln[\rho_c(\mathbf{q}_c)] \tag{14}$$

The CMD method provides a way to directly and efficiently include quantum zero–point energy and tunneling in molecular dynamics simulations. It has also been shown[18,19] that the self-diffusion constant can be calculated from CMD by studying the behavior of the centroid mean-squared displacement at long times or, equivalently, by a Green-Kubo-like relationship for the centroid velocity correlation function according to the CMD equivalents of Equations 2 and 3.

One remarkable feature of CMD is that it allows quantum particle motion to be studied with a numerical effort that scales with system size in the same way as a classical MD simulation.[20] Therefore, the dynamics of quantized particles in general many-body systems can now be simulated without having to solve the many-body time-dependent Schrödinger equation. A number of powerful and flexible algorithms for solving the basic CMD equations have also been developed.[20] This task is not entirely trivial, since the centroid potential $V_c(\mathbf{q}_c)$ in Equation 14 is a kind of quantum potential of mean force that seemingly requires an equilibrium path integral averaging over the fixed-centroid path fluctuations at each timestep. A "direct" algorithm[20] for

8

integrating the CMD equations, which performs "on the fly" the statistical averaging implicit in the centroid force calculation, combines MD with MC moves. In this approach, the "natural" CMD timestep, being on par with the timestep in the classical limit, is broken into N_{MC} smaller timesteps. At each of these centroid configurations, a pass of pairwise MC moves of the quasiparticles is carried out to sample the discretized path configurations while enforcing the centroid constraint. The centroid forces are then computed and the centroids moved according to those forces within the velocity Verlet algorithm for the small timestep. This algorithm has proven to be efficient for numerically solving the CMD equations.

2.2 Path Integral Simulations of Impurity Trapping and Spectroscopy in Quantum Solids, Liquids, and Clusters

Experiments at Phillips Laboratory, Edwards AFB, have demonstrated that a low concentration of lithium atoms can be metastably trapped in both solid H_2 and D_2 in the temperature range $T < 5$ K.[1,2] This is of interest because the ability of hydrogen to act as a rocket fuel might be significantly enhanced if small quantities of such light impurities are introduced into the system. To better understand the properties of such metastable quantum "alloys," it was a priority to characterize the trapping sites of individual lithium atoms in the solid hydrogen matrix.

As a first step, PIMC studies of solid,[23,24] liquid,[28] and cluster[29,30] para-hydrogen and ortho-deuterium were performed using a constant pressure version of the path integral formulation described in the previous section. A semi-empirical intermolecular pair potential, which had been obtained by others a number of years ago through a fitting to solid state data,[48] was used in our studies for the hydrogen. This potential gives a rather good account of pV compression data. [It should be noted that a pressure of only 200 MPa (2 kbar) is sufficient to change the molar volume of solid hydrogen from 23.2 cc/mol to ca. 17 cc/mol.] The calculated energy and molar volume of the hydrogen liquid from the PIMC simulations were found to be in excellent agreement with experiments for temperatures ranging from the triple point up to the boiling point. These results justified the choice of the intermolecular potential used in the simulations, as well as the computational methodology.

Once the reliability of the PIMC code had been established for the case of solid and liquid hydrogen, the simulation effort focused on a lithium atom impurity immersed in bulk liquid[26] and solid[25] para-hydrogen, as well as ortho-deuterium. A question first arose as to the potential for the lithium (guest) – hydrogen (host) interaction. A lithium-hydrogen pair potential was constructed by fitting the results of ab initio quantum chemical calculations and is shown in Figure 3. This procedure has since been further refined.
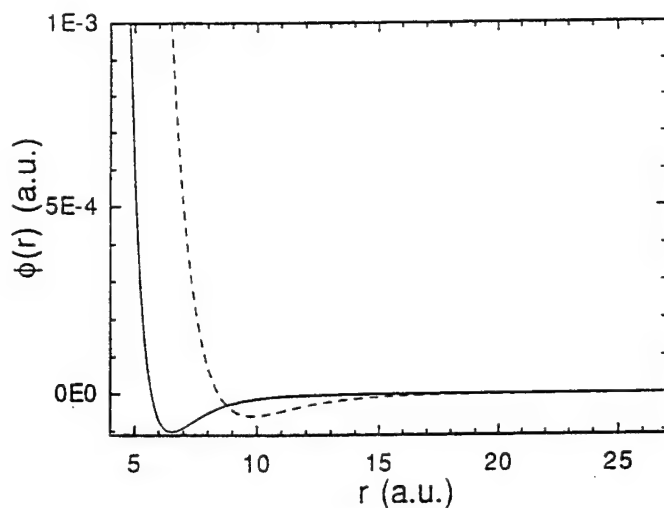
Figure 3
A Comparison of the H_2-H_2 and $Li-H_2$ Empirical Pair Potentials Employed
in the PIMC Simulations of a Li Impurity in a Solid $p-H_2$ Host

Since an isolated lithium atom is much larger than the host hydrogen molecules, trapping sites consisting of one to six vacancies in the hydrogen lattice were investigated (see Fig. 4). Interestingly, all of the sites were found to be comparable in energy. This is due to the large compressibility of para-hydrogen and ortho-deuterium solids, which permits the lattice to relax to comfortably accommodate the impurity.
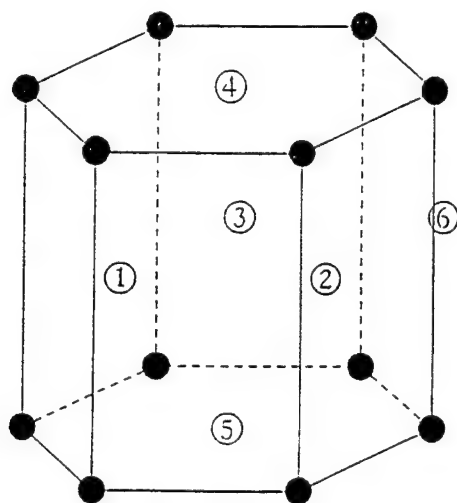
Figure 4
A Schematic Showing Various H_2 Molecules Which can be Removed
from hcp $p-H_2$ Lattice to Accommodate an Atomic Li Impurity

The numbering in Figure 4 refers to the number of hydrogen vacancies and their position.

10

The treatment of any system consisting of an impurity plus a solid with vacancies requires some care. The presence of the vacancies can give rise to a number of different local minima in the solid that can trap the impurity. These minima can be separated by large barriers that are difficult to overcome on the "time scale" of a Monte Carlo simulation. Therefore, a relatively simple and unbiased PIMC method was developed for the determination of the likely configurations of vacancies bound to the lithium impurity in the para-hydrogen or ortho-deuterium systems.[25] In one of the earlier studies,[27] a lithium impurity in liquid para-hydrogen at $T = 14–20$ K was investigated (Fig. 5). For such a liquid, the relevant configurations could be sampled efficiently, and the solvation shell of the lithium impurity was found to consist of approximately 20 molecules (Fig. 6). Several configurations of the "solvated" lithium atom and its first 20 neighbors in the liquid were then saved for subsequent use. We refer to such configurations as "liquid cores." A trapping site in the hydrogen solid was then prepared using the liquid cores in the following manner. An arbitrary point in an equilibrated neat solid configuration was chosen and $20+n_v$ molecules removed. The liquid core was then inserted into the solid and a constant pressure PIMC simulation commenced. Equilibration to a relaxed impurity "implantation" configuration was found to be rapid (~ 5000 steps). This procedure was repeated for a number of different liquid cores and neat solid configurations. The assumption in this procedure is the physically reasonable one; i.e., that the vacancies occur only in the first neighbor shell around the lithium atom. Interestingly, for a given n_v, relatively few relaxed configurations were observed. Shown in Figures 7 and 8 are the resulting sites with $n_v = 3$ and 4 vacancies (cf. Fig. 4) that were energetically favored. These trapping sites always contain Li in asymmetric locations, i.e. shifted off the ideal interstitial or lattice sites.

The inhomogeneously broadened dipole spectra of the lithium impurity in the various sites were next calculated[25] and compared to the experimental results of Fajardo.[1,2] This was accomplished by taking equilibrium configurations from the constant pressure PIMC runs, replacing the empirical lithium atom with an electron and a lithium ion core, both of which interact with the hydrogen host through pseudopotentials, and then determining the electronic states using a radial fast Fourier Transform Lanczos method.[27] The spectra for Li in various sites of the hydrogen solid are shown in Figure 9. This approach accounts for the zero-point motion and thermal effects present in the system. Based on these calculations, lithium atoms were suggested to preferentially occupy a three-vacancy trapping site in para-hydrogen, while in ortho-deuterium a four-vacancy trapping site seems to be favored. Interestingly, the high energy tail of the experimental spectrum is underestimated in all of the calculations. The "average" energy of this tail region suggests that it may in fact be caused by a rotational ($J = 0 \rightarrow 2$) Franck–Condon transition in the neighboring hydrogen molecules; such effects have been neglected in the simulation but could be included in the future through an explicit treatment of the hydrogen rotations.
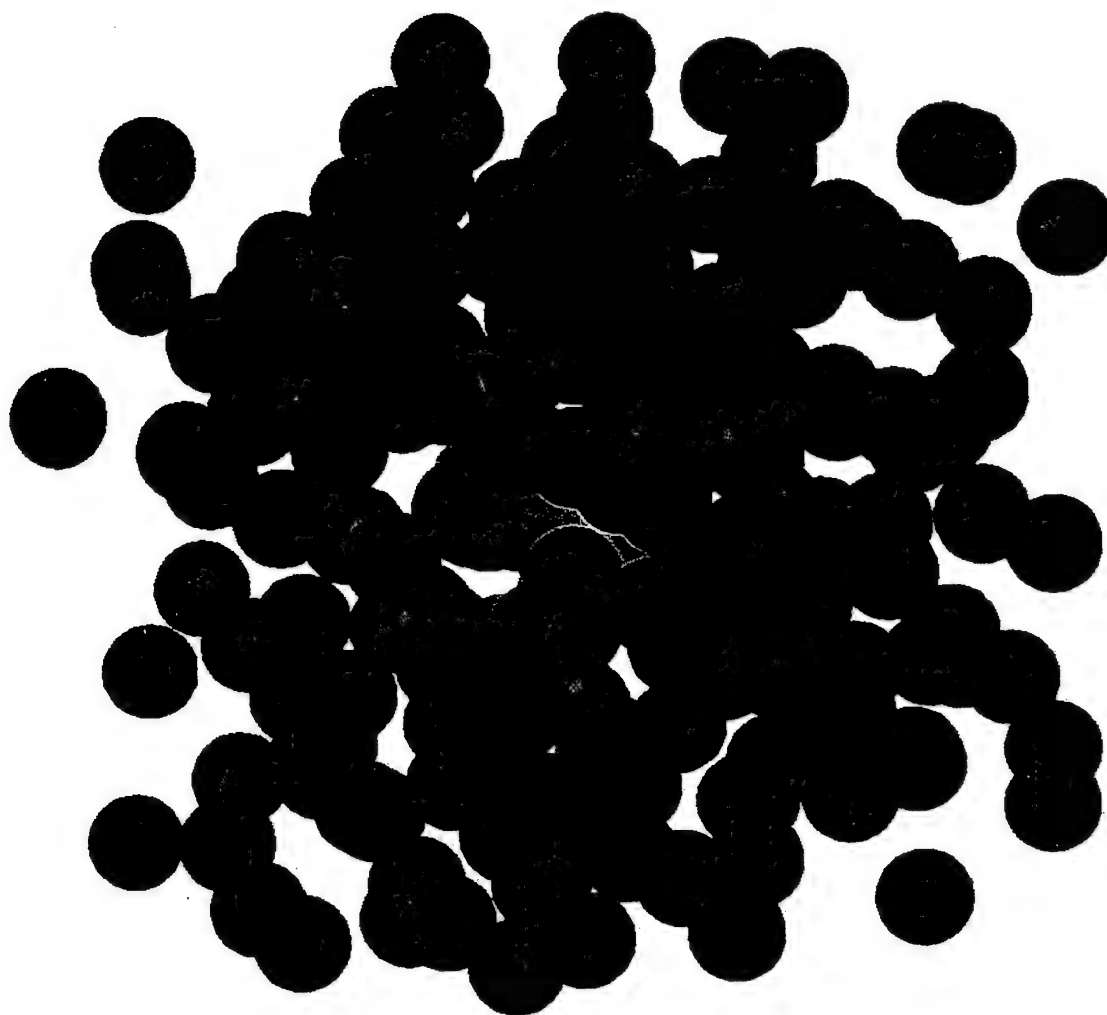
Figure 5
A Snapshot Taken from a Constant Pressure PIMC Calculation
of a Lithium Atom in Liquid Hydrogen

Each blue sphere in Figure 5 represents a para-hydrogen molecule and the larger yellow ball the lithium impurity. The closest 20 neighbors to the impurity are colored light blue. The latter constitute the "liquid core" that is "implanted" into hcp solid hydrogen as a means of searching for the possible trapping sites of ablated lithium atoms.
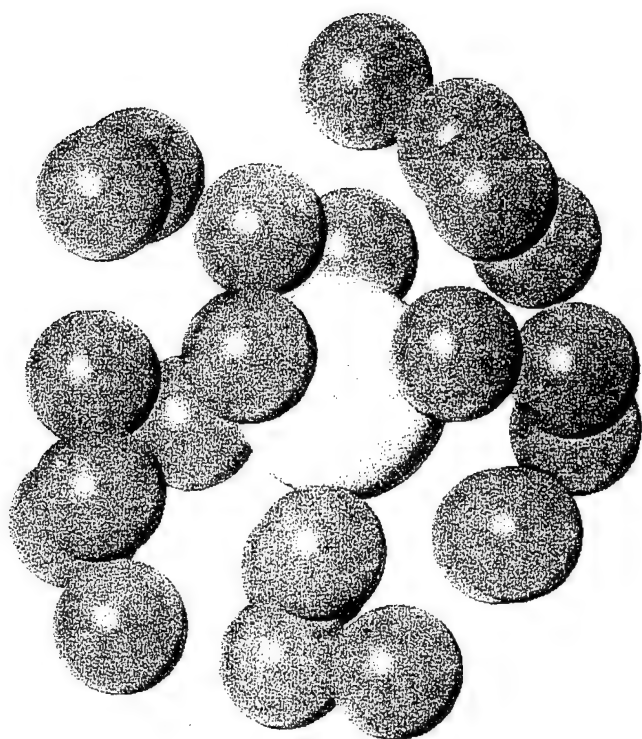
Figure 6
The Solvation Shell of the Lithium Impurity in Liquid Para-
Hydrogen Consisting of Approximately 20 Hydrogen Molecules
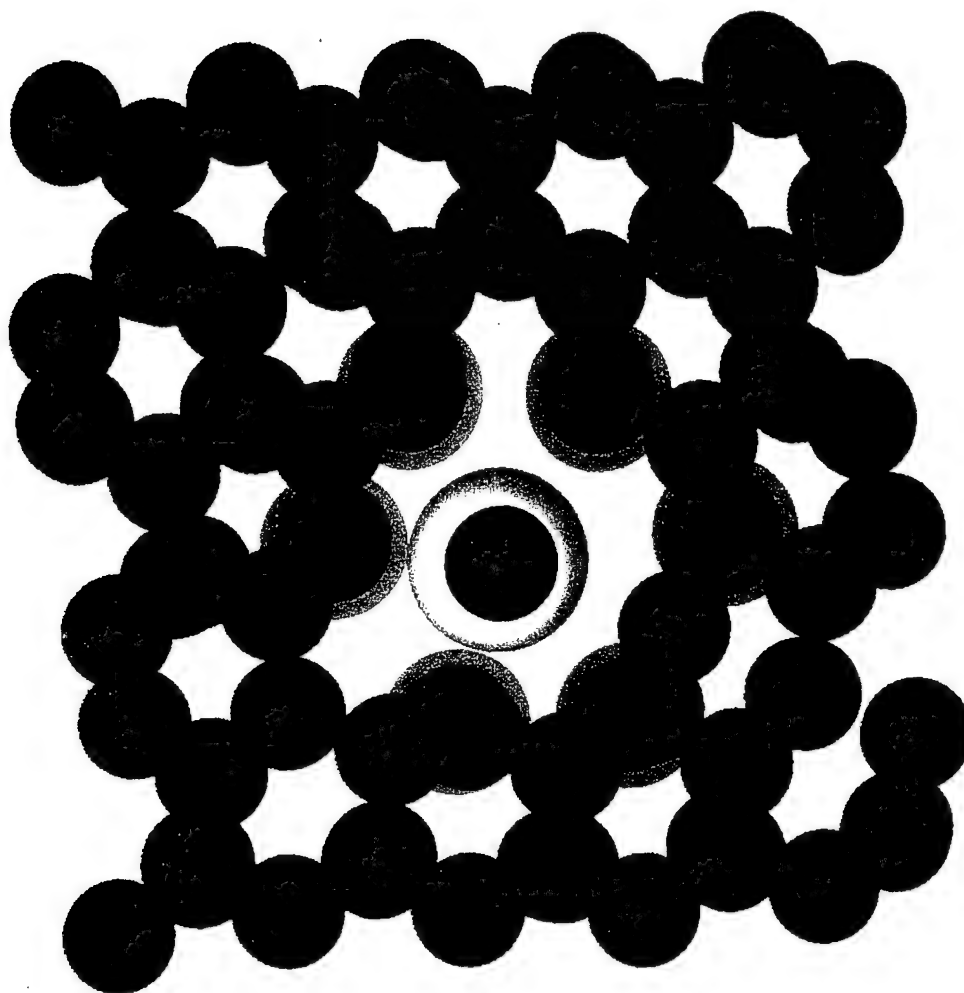
Figure 7
Top View of a Configuration Taken from a Constant Pressure PIMC
Calculation of a Lithium Atom Trapping Site in Solid Hydrogen

The impurity site in Figure 7 was created by first removing 23 host-lattice hydrogen molecules and then "implanting" a "liquid core" consisting of a single lithium atom and 20 hydrogen molecules. The asymmetric location of the lithium atom in an otherwise perfect hexagonal lattice with three vacant sites was the result of the constant pressure PIMC calculation.
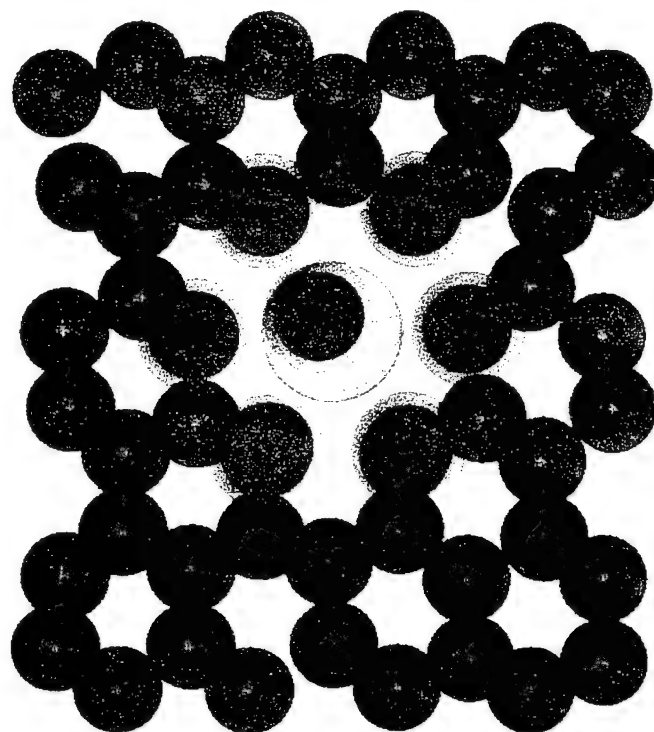
Figure 8
Top View of a Configuration Taken from a Constant Pressure PIMC
Calculation of a Lithium Atom Trapping Site in Solid Hydrogen

The impurity site in Figure 8 was created by first removing 24 host-lattice hydrogen molecules and then "implanting" a "liquid core" consisting of a single lithium atom and 20 hydrogen molecules. The asymmetric location of the lithium atom in an otherwise perfect hexagonal lattice with four vacant sites was the result of the constant pressure PIMC calculation.
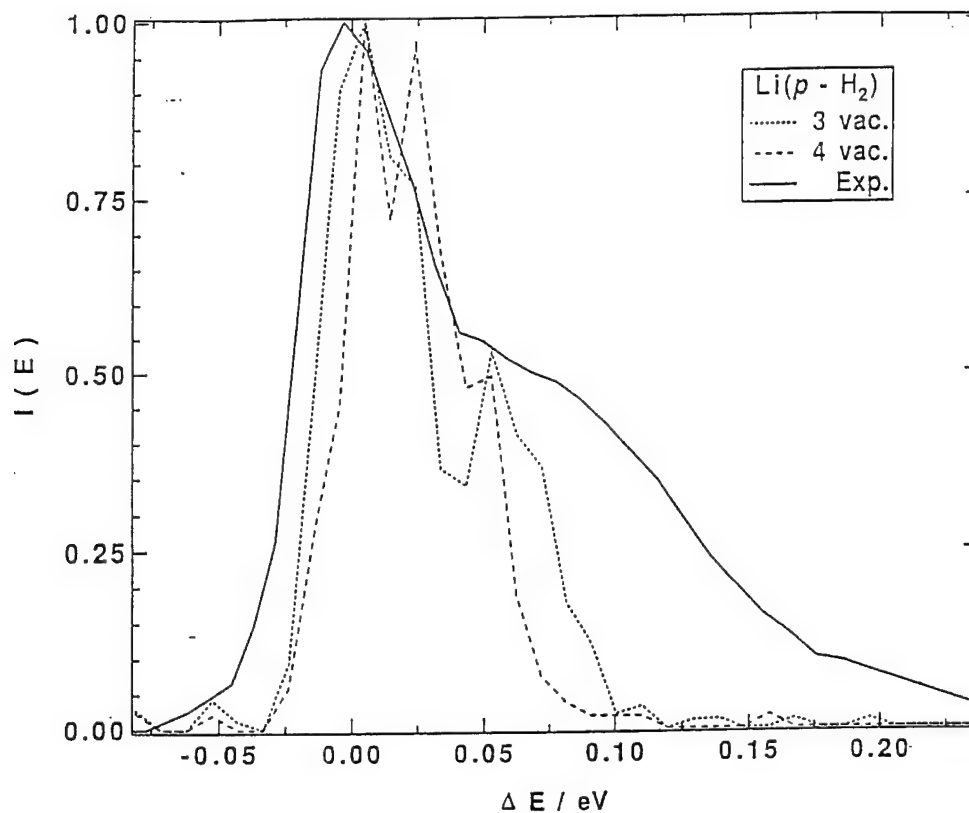
Figure 9
The Calculated Dipole Spectrum of a Lithium Atom in Solid Para-Hydrogen at T = 4 K for Various Trapping Sites

The trapping sites (cf. Figs. 3, 6 and 7) are compared above to the experimental data of Fajardo.[1,2]

Complementary calculations on the Li/H$_2$ system were performed using the variational quantum Einstein model[23] for selected trapping sites (see Section 2.3, Theoretical Description of Impurities in Solid Hydrogen). Based on free energy considerations, it was found that the Einstein model favors the four-vacancy site in both para-hydrogen and in ortho-deuterium. Since the Einstein model is a local harmonic one, its difference from the simulation results illustrates the importance of anharmonic, collective quantum motion in determining the structure of the impurity trapping site.

The interaction of Li with clusters containing either 12, 13, 32, 33, or 34 para-hydrogen molecules were also investigated.[27] The lithium atom was found to reside on or near the cluster surface even though the clusters were studied at much lower temperatures than the liquid; i.e., 2.5 to 6 K. Figure 10 shows representative configurations taken from the path integral calculations for the cluster with 33 para-hydrogen molecules. Although in all cases the Li atom resides on the outside of the cluster, perturbations of the structure are observed in comparison to neat para-hydrogen clusters, which were also studied.[29] For both the clusters and the neat liquid, the

inhomogeneously broadened dipole spectrum of the lithium atom was again calculated using the radial fast Fourier Transform Lanczos method. In the clusters, the spectra exhibit a main absorption band near the unperturbed atomic Li value and a second asymmetric band shifted to the blue. The latter is identified as arising from the p-orbital oriented radially towards the cluster, whereas the main band is composed of the two p-orbitals oriented parallel to the cluster surface. The spectrum of Li in the liquid is significantly broader than the cluster spectra. The ionization spectrum of Li attached to the para-hydrogen clusters was also studied. The spectra progressively red-shift and broaden from the atomic value with increasing cluster size.
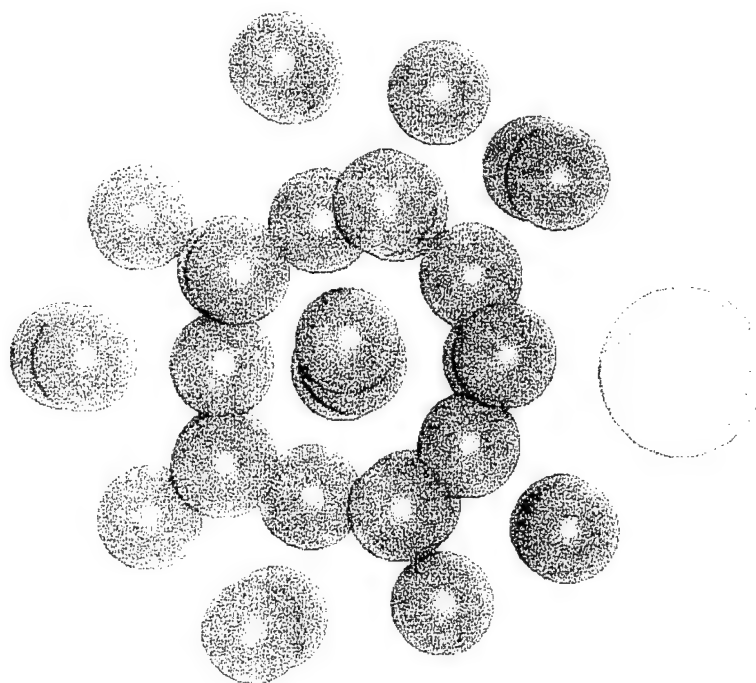
Figure 10
A Snapshot from a PIMC Simulation of the Li(p–H$_2$)$_{33}$ Cluster

In Figure 10, note the ordering of the hydrogen molecules and the fact that the lithium atom is on the surface of the cluster.

2.3 Theoretical Description of Impurities in Solid Hydrogen

Another research effort involved the development of a theoretical framework by which to characterize and understand the structure and thermodynamics of impurities in the p–H$_2$ solid.[23,24] These analytical developments were variational in nature and based on the well-known Gibbs-Bogoliubov (GB) inequality. This inequality states that the true Helmholtz free energy of a system

17

is the lower bound of the sum of the free energy for a variational "reference system" and the difference between the total energies of the exact and reference systems, averaged over the canonical ensemble generated from the reference system. Explicitly, the GB inequality is given by

$$F \leq F(\zeta) = F_{ref}(\zeta) + \langle H - H_{ref}(\zeta) \rangle_{ref} \tag{15}$$

where ζ denotes the set of variational parameters. Variational theories based on the above equation involve the specification of a suitable (and tractable!) reference Hamiltonian, which depends on one or more variational parameters, and the subsequent minimization of the right-hand side of Equation 15 with respect to those parameters.

As a first step in the theoretical analysis, a variational Einstein model for describing low temperature solids, with and without impurities, was developed from the Feynman path integral perspective.[23] The theory can be used to predict fully quantum mechanical values for the thermodynamics (e.g., free energy, entropy, internal energy, etc.) and the equilibrium structure (e.g., pair and angular correlation functions) of a solid. The independent harmonic oscillator assumption implicit in the Einstein model allows the results to be cast in a straightforward analytic form. Additionally, the path integral formulation of the model yields solutions which explicitly depend on the path integral discretization parameter P. One can thus systematically examine the equilibrium behavior of a solid, ranging from the classical to the quantum limits. The Einstein model was applied to examine the behavior of solid hydrogen and solid hydrogen containing lithium impurities.

Although the description of solid hydrogen with the path integral Einstein model agreed fairly well with simulations in the nearly classical limit, somewhat larger discrepancies were observed in the fully quantum limit.[23] This difficulty is at least partially a result of the independent harmonic oscillator assumption for the solid. Since the excitations in a quantum solid are mainly acoustic phonons, the particles' motions are expected to be strongly correlated with one another, and the independent harmonic oscillator assumption may become inappropriate to characterize solids at low temperatures. The acoustic phonons can, however, be correctly characterized by a Debye model, the parameters of which could also be determined variationally from Equation 15.

Impurities, on the other hand, destroy the translational symmetry of a solid, so the dynamical picture for a solid with impurities becomes greatly complicated. The motion of an impurity can either be localized when its vibrational frequencies are much higher than the Debye frequency, or the impurities' motion may be strongly mixed with the delocalized vibrational states if its vibrational frequencies are smaller than the Debye frequency. In general, the motions of impurities are represented by neither of those two extreme cases. The theoretical effort, therefore, turned to the development of an analytical model that bridges the two extremes and accurately accounts for the effects of impurities in a low temperature solid.[24] This new variational "mixture" model was formulated to study the effect of substitutional impurities in solids at very low temperature. Similar

18

to the Einstein model, the mixture model is a self-consistent harmonic one. In the latter model, however, except for the impurities, the deviations of all the particles from their thermodynamical equilibrium positions are assumed to arise from the vibrations of an effective harmonic system in which each particle is coupled to all others. To account for the nature of the motion of impurities, additional degrees of freedom, which are used for the localized modes, were introduced into the model. The application of the GB variational principle was carried out in the extended space in order to determine the variational parameters. The actual motions of impurities were then partitioned between the correlated motion with the lattice and the independent harmonic oscillations via a projection scheme. This theoretical analysis, which was not straightforward, effectively "mixes" the Einstein and Debye models variationally, allowing for extended lattice vibrations and arbitrarily localized impurity modes. The averaged effect of the anharmonicity in the pair potentials is included self-consistently in the variational model, and the impurities are allowed to induce structural distortions at constant pressure. The (quite accurate) predictions of the mixture model for the pair distribution function of pure $p–H_2$, and for $H-H_2$ the distribution for solid hydrogen with a substitutional atomic hydrogen impurity, are shown in Figure 11 and compared there to exact PIMC results.
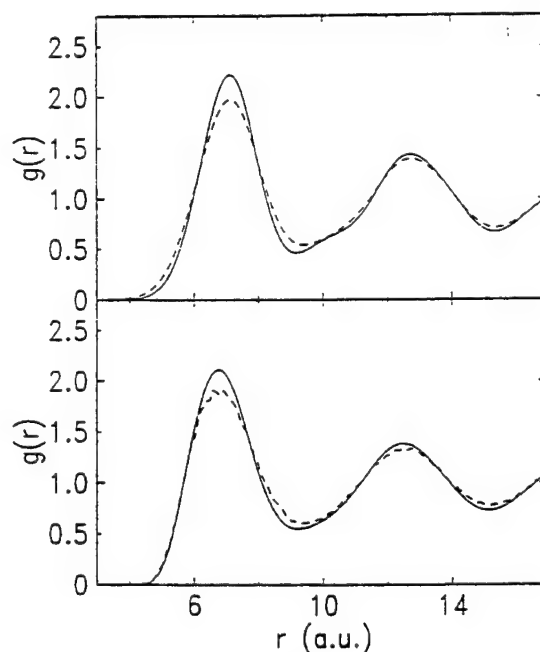
Figure 11
Pair Distribution Functions in Solid p-H_2

The top panel of Figure 11 shows the theoretical "mixture model" prediction of the $H_2–H_2$ pair distribution function (solid line) and the $H–H_2$ pair distribution function (dashed line) in a $p–$

H_2 solid with a substitutional atomic hydrogen impurity. The lower panel shows the same quantities as calculated from a PIMC simulation.

2.4 Structure and Spectroscopy of Hydrogen Atoms in Solid Molecular Hydrogen

For a number of years, there has been considerable interest in the structure and dynamics of atomic hydrogen impurities in solid hydrogen[49-56] because of their theoretical potential to significantly enhance the characteristics of rocket fuels. For example, the ESR absorption spectra of the trapped H atoms in solid hydrogen has been reported.[57] These experimental results presented a good challenge for a theoretical/computational study.[26] The main purpose of this effort was to derive a formula for the ESR linewidth that takes into account the localized nature of H atom impurity electron (Fig. 12) and the large fluctuations of the quantized nuclear configurations. The modified formula would then be employed in a first-principles calculation to study the effects of the local distortions, as well as the molecular hydrogen vibrations and rotations, on the linewidth of the ESR spectra.
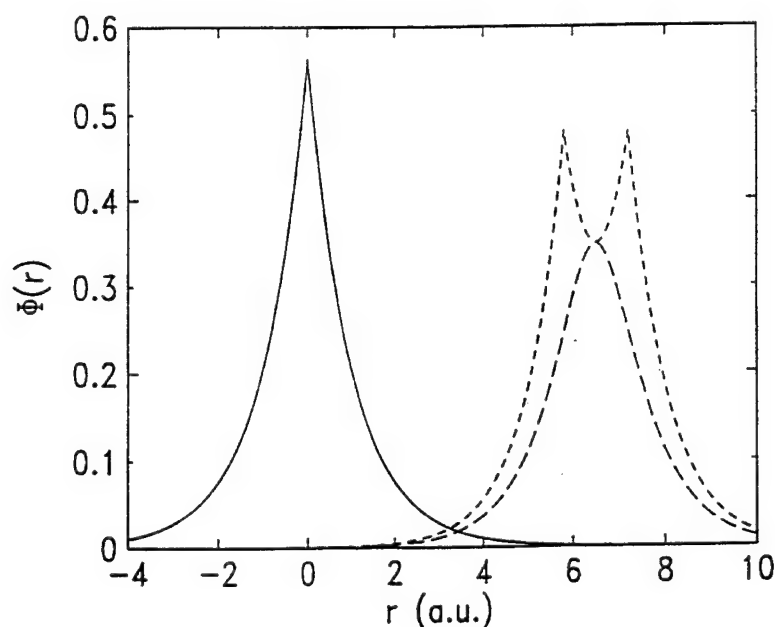
Figure 12
A Schematic Sketch of the Square of the Localized Atomic Wave Function,
$\Phi(r)$, of an H Atom and a One-Electron Wave Function of an H_2 Molecule

In Figure 12, the solid line represents the atomic wave function of the H atom, the short dashed line corresponds to an H_2 orientation parallel to the line which connects the H atom and the center of mass of the H_2 molecule, and the long dashed lines is for an H_2 orientation perpendicular to the line.

The first issue considered was the nature of the electronic wave function of the trapped impurity. When an H atom is trapped in solid hydrogen, according to the Pauli principle, its atomic wave function must adjust itself to avoid overlap with the wave functions of the molecular H_2 electrons that have the same spin (the molecular orbitals of the solid molecules must change as well). Based on the requirement that the total electronic energy must be a minimum, an equation was derived from Hartree's self-consistent field theory to uniquely determine the orthogonalization of atomic orbitals (Fig. 13). Then, based on the perspective that hyperfine interactions between the electron of the impurity and the nuclear moments of adjacent particles lead to the ESR linewidth, a formula was derived that includes the ensemble average over the quantized nuclear configurations.[26]
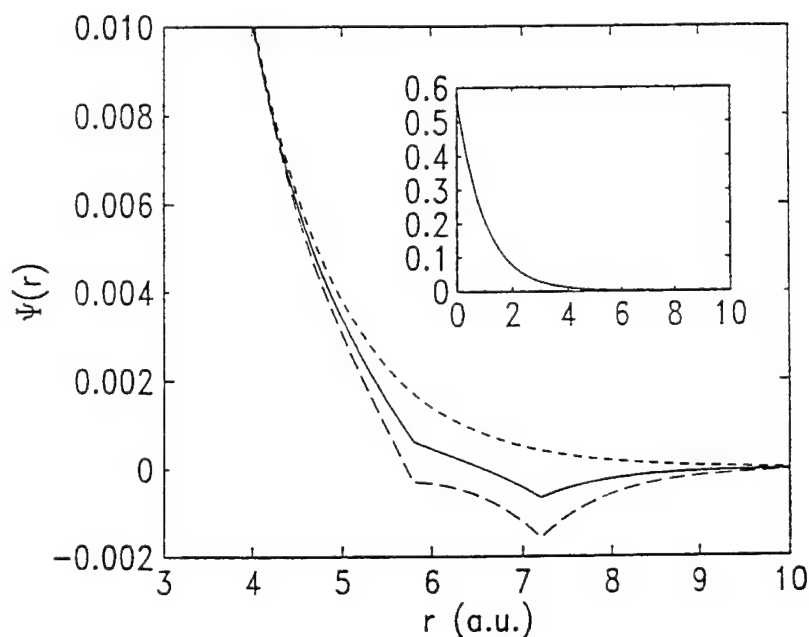
Figure 13
The Correction of the Atomic Wave Function, $\Phi(r)$, for an H Atom Caused by the Presence of an H_2 Molecule

In Figure 13, the H_2 molecule is R = 6.5 atomic units (a.u.) away with its orientation pointing toward the H atom. The solid line corresponds to our rigorous orthogonalization procedure, while the long dashed line is the atomic wave function obtained when an approximate Gram-Schmidt orthogonalization is used. The short dashed line is the original zeroth-order atomic wave function. Note the anti-bonding-like behavior of the orthogonalized hydrogen wavefunction.

The newly derived formula was then employed in the computation of the linewidths of the ESR spectra for impurities trapped in substitutional and interstitial sites in solid hydrogen. The nuclear configurations were generated from constant pressure PIMC simulations. The numerical calculations showed that the inclusion of zero-point vibrations drastically increased the linewidth of

21

the ESR spectra over the linewidth calculated simply from the average equilibrium configuration. From the simulations, it was also found that an H atom in an interstitial site will effectively push its nearest neighbors outward. More importantly, when the quantum effects of the solid are fully taken into account, the lattice is not able to maintain the cavity of the interstitial impurity, and the local structure around the impurity becomes the same as that for a substitutional impurity (Fig. 14). Because of this large structural relaxation, the linewidth for the H atom trapped at interstitial sites decreases to the same value as that for an H atom trapped in substitutional sites. The calculated ESR linewidth in either site was found to be in virtually exact agreement with the experimental result of 0.34 G. This conclusion remains unchanged when a pressure as high as 10 kbar is applied to the solid. Since the observed lattice relaxation and calculated linewidths suggest that all trapping sites become essentially equivalent (i.e., somewhat like a fluid), this theoretical study may cast some doubt on the ability to trap and stabilize a significant mol fraction of atomic hydrogen impurity in solid p–H_2.
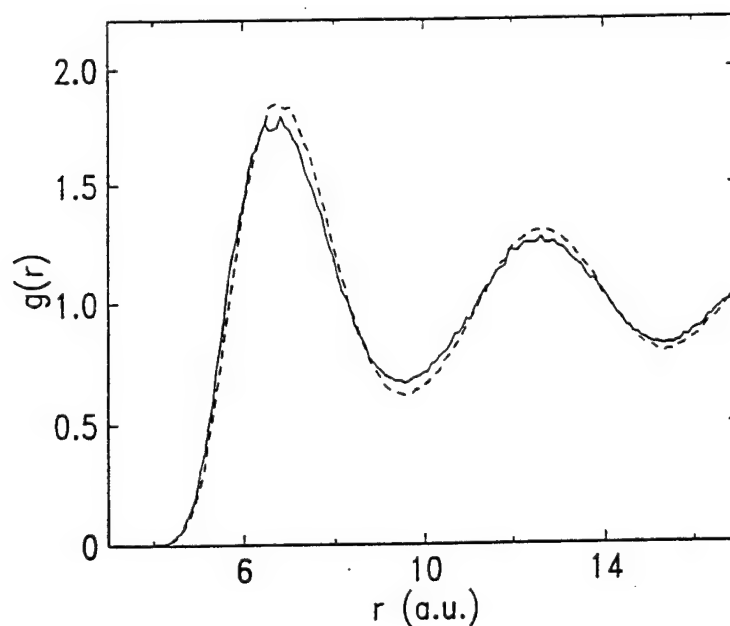

Figure 14
A Comparison of the Pair Correlation Function, g(r), Between
an H Atom and p–H_2 Molecules

The curve in Figure 14 was generated from a PIMC calculation at 5 K with $P = 50$ and for different initial conditions. The solid line corresponds to the H atom initially in an interstitial site while the dashed line is for it in a substitutional site.

22

2.5 Centroid Molecular Dynamics Algorithms

To carry out the quantum dynamical CMD studies of low temperature HEDM systems, efficient and effective algorithms were needed.[21] These are described in the next paragraph.

The discretized path integral in Equation 6 converges to the true result as $P \to \infty$. In practice, a finite value of P is chosen to ensure that the quantities of interest are adequately converged. For example, solid para-hydrogen has pronounced quantum effects at the temperatures studied, and a large value of P is necessary at the lowest temperatures (i.e., $P = 50\text{-}100$ at 5 K) to obtain convergence of the dynamical and structural properties. Thus, a reasonable amount of centroid-constrained averaging is necessary at each CMD timestep to calculate the centroid force, making its calculation computationally challenging. However, this averaging lends itself to quick and efficient evaluation on a parallel computer.

Normally, for a direct CMD calculation[20] carried out in serial fashion, one PIMD (or, alternatively, PIMC) trajectory is run for the number of time steps, M, to evaluate the centroid force at each CMD timestep (M is chosen based on convergence issues).[20] In the HPCMD implementation,[21] the centroid force is calculated in parallel by averaging m independent PIMD trajectories, and each trajectory is run for M/m timesteps (Fig. 15). In addition to being faster, this procedure in principle samples phase space more efficiently than the traditional method of evaluating the centroid force with a single PIMD simulation because the configurations are not as highly correlated. Each PIMD centroid averaging trajectory is started from the same initial quasiparticle configuration, but the velocities are randomized at the beginning of the simulation. A
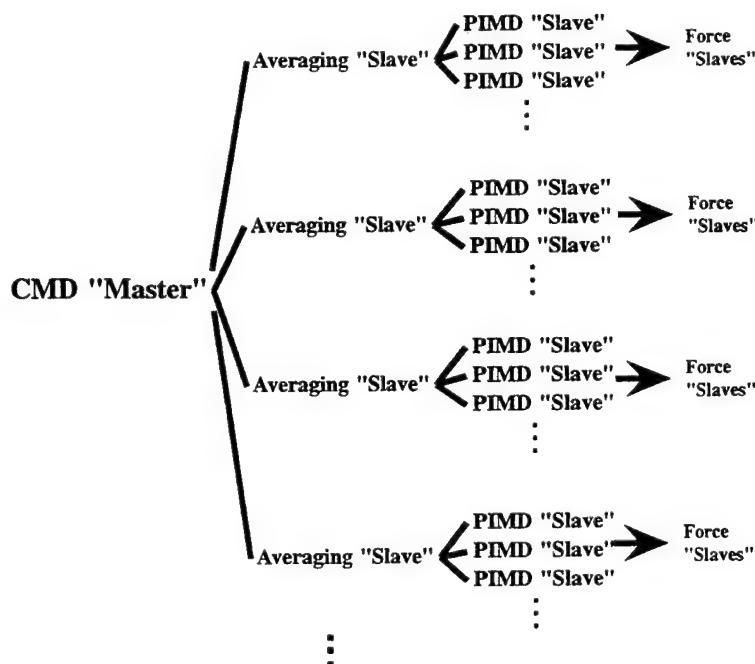

Figure 15
A Schematic Flow Diagram of the Parallelism Inherent in the
Hyper-Parallel CMD (HPCMD) Algorithm

23

Nosé chain can be linked to the centroid-constrained quasiparticles in PIMD to ensure ergodic sampling[58,59] (chains of length two have been used for each hydrogen molecule). Alternatively, a staging PIMC algorithm can be used for the centroid force averaging, as originally described in Reference 20, which can lead to more rapid convergence of the force.[58,59]

The method of running independent trajectories in parallel to obtain the centroid force is termed the "first tier" of parallelism in HPCMD. This part of the algorithm can be run over any number of processors on a parallel computer, up to the point where one PIMD timestep is run per processor node, which is the maximum division of labor over M processors, at this level. As outlined in Reference 21, the number of timesteps M can be adjusted to test convergence of the centroid force and the uniqueness of the centroid trajectories.

As a result of this parallelism, each PIMD simulation does M/m PIMD timesteps to evaluate the centroid force, but each one of these timesteps can also be done in a parallel manner over imaginary time slices with minimal inter-node communication and perfect load balancing (cf. Fig. 15). Since each trajectory has N physical particles, and each of these is discretized into P equivalent quasiparticles, the overall force calculation scales approximately as $N^2 \times P$ (or less, depending upon the range of the interactions). Thus, the obvious parallel solution is to evaluate the intermolecular forces (often 99% of the computational effort) for each imaginary time slice in parallel at each PIMD timestep. This parallel evaluation of the intermolecular force at each PIMD step is termed the "second tier" of hyper-parallelism. This tier of the algorithm can be run on any number of processors up to a total of P, the number of imaginary time slices. It is most efficient when P is an integer multiple of the number of processors.

With the two levels of parallelism just outlined, the CMD calculation can be run over $M \times P$ processors. Therefore, the maximum division of labor is when all M PIMD calculations of the centroid force at each CMD timestep are done on separate processors, and in turn all P imaginary time slices for each PIMD calculation are done on P separate processors. In practice, however, this degree of parallelism may not always be utilized because of the limited number of processors available.

A "third tier" of hyper-parallelism is even possible for very large systems (cf. Fig. 15). The parallel evaluation of the intermolecular force for each PIMD step can still be an N^2 problem at each imaginary time slice for longer-ranged forces. This force evaluation can be done in parallel, but because of inter-node communication bottlenecks, this is only efficient for large systems (i.e., usually 1000 particles or more). This force loop parallelism has been implemented in other studies[60,61] but not yet in the para-hydrogen system, as the intermolecular force problem is not exceptionally expensive until the number of particles reaches many thousand.

Benchmarks of the HPCMD algorithm were carried out for liquid para–hydrogen on an IBM SP2. The performance and scalability of the algorithm is shown in Figure 16. The plot of speedup

versus number of processors on the SP2 was almost linear over a range from 1 to 64 nodes. On an IBM 590 (one wide node of the SP2), the serial version of the code performed at 70 million floating point operations per second (MFLOPS), while on the Cray C90 the serial version of the code ran at 280 MFLOPS. In contrast, the parallel code ran at approximately 3.1 GFLOPS over 64 nodes. At this speed, the code utilized the parallel CPU array with about an 80% efficiency (real speedup/maximum theoretical speedup), and it ran more than 10 times as fast as the single processor on a Cray C90. The simulations given in Figure 16 were carried out for 1440 particles, and the efficiency would clearly increase with larger system sizes. It is anticipated that for very large hydrogen systems, a HPCMD code could be developed that achieves 50-100 GFLOPS performance on a current-generation IBM SP2.
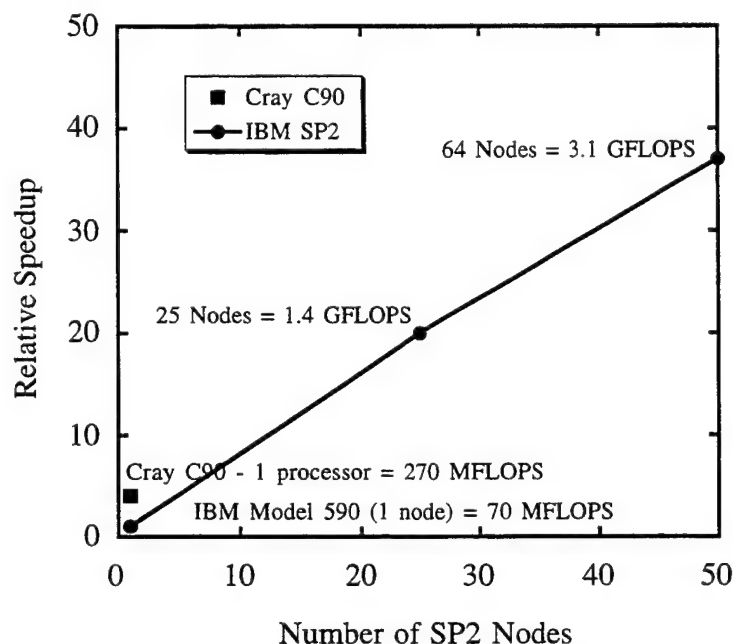
Figure 16
The Scaling of the HPCMD Algorithm with Number of Parallel Nodes on an IBM SP2 Computer

The test simulation in Figure 16 was for liquid p–H_2 at 14 K with 1440 molecules in the simulation cell.

2.6 Quantum Dynamical Simulations of Liquid Hydrogen

As an early test of the HPCMD algorithm, velocity auto-correlation functions, $C_{vv}(t)$, for liquid para–hydrogen were computed.[21,22] The pair potential for the interparticle interactions was taken to be that of Silvera and Goldman.[48] The path integral was discretized into $P = 16$

25

quasiparticles at 25 K, while at 14 K it was found that $P = 50$ was necessary for the structural properties to be well converged.[24,25] In the correlation function calculations, it was found that 180 periodically replicated hydrogen molecules were adequate for convergence with system size.

At 25 K, independent trajectories with lengths of 4, 6, 8, and 20 ps were used to test the convergence of $C_{vv}(t)$. There were only minor differences between the correlation function computed from an average of two 8 ps trajectories and that computed from a 20 ps trajectory. The velocity correlation function is shown in Figure 17. The converged CMD self-diffusion constant was calculated from the average of two 8 ps trajectories. The CMD method reproduced the experimental self-diffusion constant quite well (1.54 $\pm$ 0.1 Å^2/ps versus 1.6 Å^2/ps experimentally). The classical MD result in which a constant pressure classical MD simulation was first used to equilibrate the system volume[24,25] is given by 0.5 $\pm$ 0.05 Å^2/ps, so the quantum effects are significant even at this temperature.
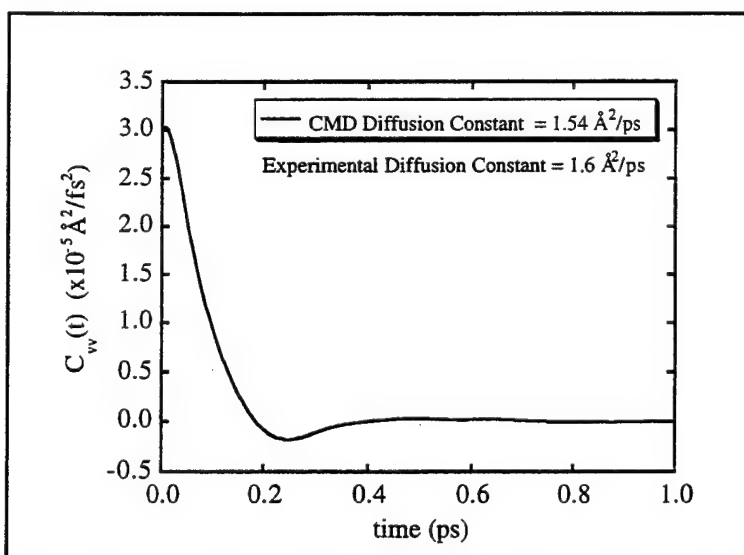
Figure 17
Plot of the CMD Velocity Auto-Correlation Functions for Liquid
p-H$_2$ at 25 K and V = 31.7 cm^3 mol^{-1}

The quantum CMD value of the self-diffusion constant is found to be 1.54 Å^2 ps^{-1}, while the experimental value is 1.6 Å^2 ps^{-1}. Calculations at other densities give similar agreement between CMD and experiment.

At 14 K, two 9.8 ps HPCMD trajectories were run. A serial calculation of these trajectories by direct CMD was problematical for a reasonable turnaround time because of the number of quasiparticles and the amount of averaging required to calculate the centroid force at each timestep. By contrast, the HPCMD simulation was carried out over 25 to 64 nodes of an IBM SP2 over the course of one week. The diffusion constant of 0.32 $\pm$ 0.05 Å^2/ps as calculated by HPCMD was

somewhat lower than the experimental value of 0.4 Å²/ps, but this deviation may well be attributed to minor inaccuracies in the pair potential and not necessarily inaccuracies in the CMD methodology. The classical system was a solid at this temperature. The preliminary CMD simulations of liquid hydrogen systems have helped to establish the validity of both the theoretical and computational CMD methodology.[21,22]

The second approach for carrying out large-scale CMD simulations involved the development of effective classical-like pair potentials for the centroid variables.[20,22] In this case, the full many-body centroid potential $V_c(\mathbf{q}_c)$ for N particles was approximated as

$$V_c(\mathbf{q}_c) \approx \sum_{i=1}^{N} \sum_{j>i}^{N} v_{c,ij}(r_{c,ij}) \tag{16}$$

where $v_{c,ij}(r_{c,ij})$ was some effective centroid pair potential as a function of the distance between the quantum path centroids of two atomic sites i and j; i.e., $r_{c,ij} = |\mathbf{r}_{c,i} - \mathbf{r}_{c,j}|$. For a simple pair of particles, the quantum centroid pair potentials can be calculated directly by performing a numerical path integral calculation; i.e.,

$$exp[-\beta v^0_{c,ij}(r_{c,ij})] \equiv \frac{\int \cdots \int D\mathbf{q}_i(\tau)D\mathbf{q}_j(\tau)\delta(r_{c,ij} - \tilde{r}_{ij})exp\{-S[\mathbf{q}_i(\tau),\mathbf{q}_j(\tau)]/\hbar\}}{\int \cdots \int D\mathbf{q}_i(\tau)D\mathbf{q}_j(\tau)\delta(r_{c,ij} - \tilde{r}_{ij})exp\{-S_{fp}[\mathbf{q}_j(\tau),\mathbf{q}_j(\tau)]/\hbar\}} \tag{17}$$

where $S[\mathbf{q}_i(\tau),\mathbf{q}_j(\tau)]$ and $S_{fp}[\mathbf{q}_j(\tau),\mathbf{q}_j(\tau)]$ are the action functionals for the interacting and free particle limits, respectively. The pair separation centroid $\tilde{r}_{ij}$ in Equation 17 is given by

$$\tilde{r}_{ij} = \frac{1}{\hbar\beta} \int_0^{\hbar\beta} d\tau \left|\mathbf{q}_i(\tau) - \mathbf{q}_j(\tau)\right| \tag{18}$$

The behavior of the centroid pair potential provided insight into the origin of the dominant quantum effects in the solid through a direct comparison with the classical pair potential (see Fig. 18 for p–H_2).[22]

2.7 Quantum Dynamical Simulations of Solid Hydrogen

Historically, there has been much interest, both experimentally and theoretically, in the low temperature properties of solid hydrogen.[15,16] This interest may be attributed in part to its intrinsic value as one of the prime examples of a quantum solid, and to its practical value as a HEDM. Theoretically and computationally, the thermodynamic properties of the system have been studied by path integral simulations,[23-25,40] and the results agree very well with experiment.

A CMD calculation was carried out to directly determine the phonon spectrum of pure bulk solid para–hydrogen for the first time.[62] The Silvera-Goldman intermolecular pair potential, which had been shown to yield accurate results in previous simulations, was again employed,[47] so the H_2 molecule was described as a spherically symmetric particle with no internal degrees of freedom. This approximation is appropriate, since at the temperature studied (4 K), each hydrogen molecule

was frozen into its ground vibrational and rotational state. The ground rotational state for p–H_2 is J = 0 (J is a good quantum number even in the condensed phase system), which is spherically symmetric.

The PIMC and PIMD simulations gave a value for the density at zero pressure that compared very favorably with the experimental value (versus the classical MD result, which was 20% in error). It should be noted that classical simulations at the experimental density gave quite unphysical results (the hydrogen molecules condensed into part of the simulation cell, leaving a vacuum region). Also, the hydrogen molecules were very delocalized because of zero–point energy. The RMS width of the single particle distribution function was 18% of the lattice spacing,[25] which was also what PIMC and PIMD simulations predicted.
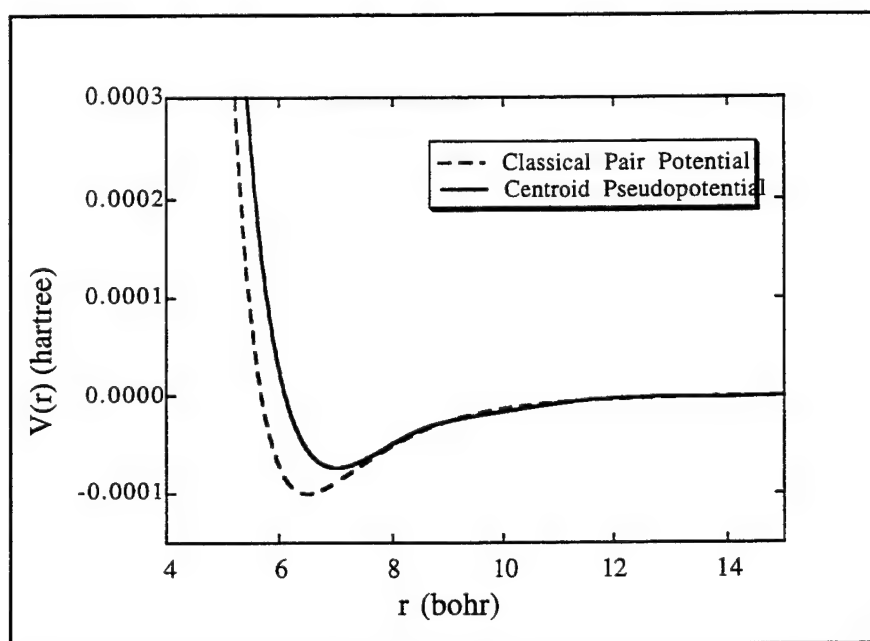
Figure 18
A Comparison of the Classical Silvera-Goldman Pair Potential
for p–H_2 with the Effective Quantum Centroid Pair Potential
Obtained Numerically at 25 K

The shallowness of the centroid potential in Figure 18 effectively reflects the zero-point quantization of the hydrogen molecules, while its minimum is shifted outward from the combined effect of the quantization and the potential anharmonicity.

The quantum velocity autocorrelation functions calculated from CMD for the solid at 4 K and the liquid at 14 K and 25 K are shown in Figure 19. Note the oscillatory behavior of the function at 4 K, which is characteristic of a solid. Classically, the zero time value of the velocity autocorrelation function is proportional to the average temperature. This is not the case quantum mechanically, because zero–point energy is included as well, which is temperature independent. It

should be noted that PIMC was chosen as the method for calculating the centroid force for the solid hydrogen CMD simulations because it proved to be more efficient than PIMD.
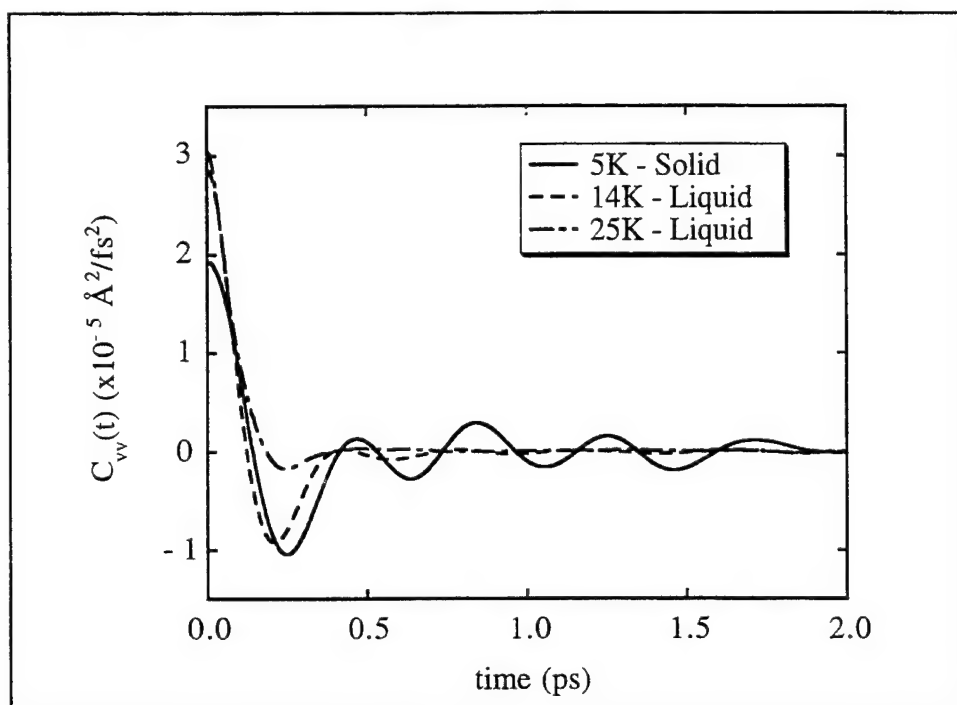
Figure 19
A Plot of the CMD Velocity Correlation Functions for p–H_2 for the Solid and Liquid at Two Temperatures

The Fourier transform of the velocity auto-correlation function from CMD is shown in Figure 20. This function can be related to the peak positions in the experimental phonon spectrum as determined from neutron scattering or infrared data. The CMD calculations agreed remarkably well with the experimental results. The CMD calculation assumed nothing about the structural form of the lattice and invoked no approximate functional form for the phonon motions. It was purely the result of a many–body quantum dynamical simulation.[62]

2.8 Lithium Impurity Trapping in Solid Hydrogen

At the time of this report, work is underway to study the actual quantum dynamics of the recombination of two lithium impurity atoms trapped in bulk solid hydrogen using CMD. There is a large thermodynamic driving force for the separated atoms to form the Li–Li dimer species, but the atoms remain separated because of the rigidity of the intervening hydrogen molecules. As with other low temperature hydrogen systems, a classical mechanical treatment of the problem is completely inadequate.

29

Figure 20
The Phonon Density of States for Solid p–H_2 at 4 K

The density of states in Figure 20 was calculated from the Fourier transform of the CMD velocity correlation function from Figure 19.

The (preliminary) centroid potential of mean force (CPMF) as a function of the relative separation of two lithium atoms in solid *para*–hydrogen at 4 K is shown in Figure 21. This quantity was computed from 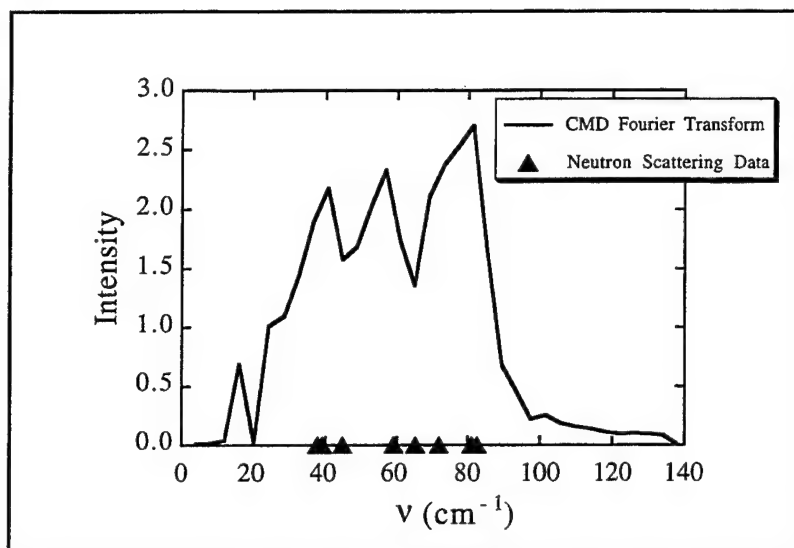a constant volume PIMD simulation. The initial configuration was equilibrated with constant pressure PIMD (zero external pressure) with the lithium atoms well separated in the lattice in single substitutional defects (top panel in Fig. 22). In these defects, the lithium atoms had equilibrium positions at the hydrogen lattice positions. The surrounding lattice of hydrogen was distorted because of the larger size of a lithium atom (relative to the hydrogen molecules), but it still maintained the basic hexagonal close packed (hcp) arrangement. Once the system was equilibrated, the volume was fixed to the equilibrium volume at zero external pressure, and the lithium-lithium centroid distance was holonomically constrained. The mean force on the lithium atoms along the lithium-lithium axis was then averaged for 75 ps. This calculation was done for the entire range of lithium–lithium separations allowed within the finite simulation volume (see lower panel of Fig. 22 for the barrier configuration). The integrated result of these calculations in Figure 21 (i.e., the CPMF) gives a direct estimate of the quantum barrier for the recombination of the lithium atoms. This barrier was rather high ($\approx$ 130 K). In fact, the barrier was over 30 times the thermal energy for the system, which means the lithium atom recombination was a rare (or activated) event. The height of this calculated barrier seems encouraging for the possibility of stabilizing lithium impurities in solid hydrogen.

At the time of this report, a dynamical estimate of the prefactor for the quantum transition state theory (TST) rate constant is being computed by CMD. In this calculation, the lithium atoms

30

are equilibrated at a relative separation such that they are in the well of the CPMF at 12.8 Å apart. The period of motion for the relative lithium–lithium distance can then be determined from the CMD trajectories.
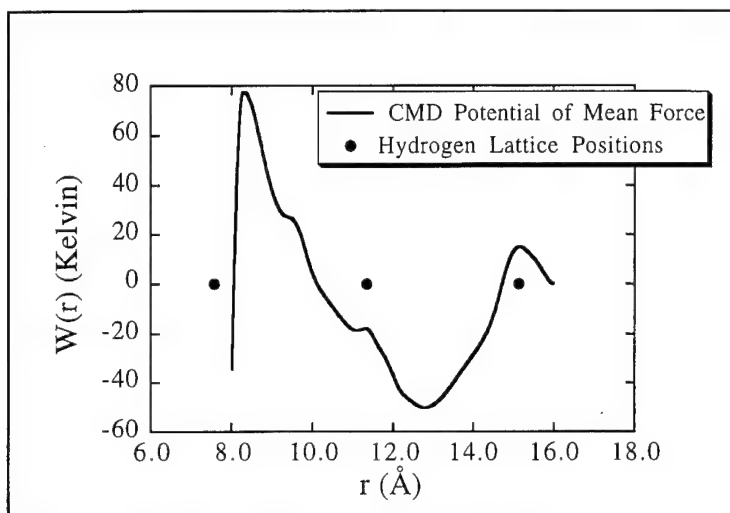
Figure 21
The Potential of Mean Force Between Two Atomic Lithium
Impurities in the Solid _p_-H₂ Lattice at 4 K

The error bars in Figure 21 are on the order of 10 K. The barrier height is approximately 130 K.
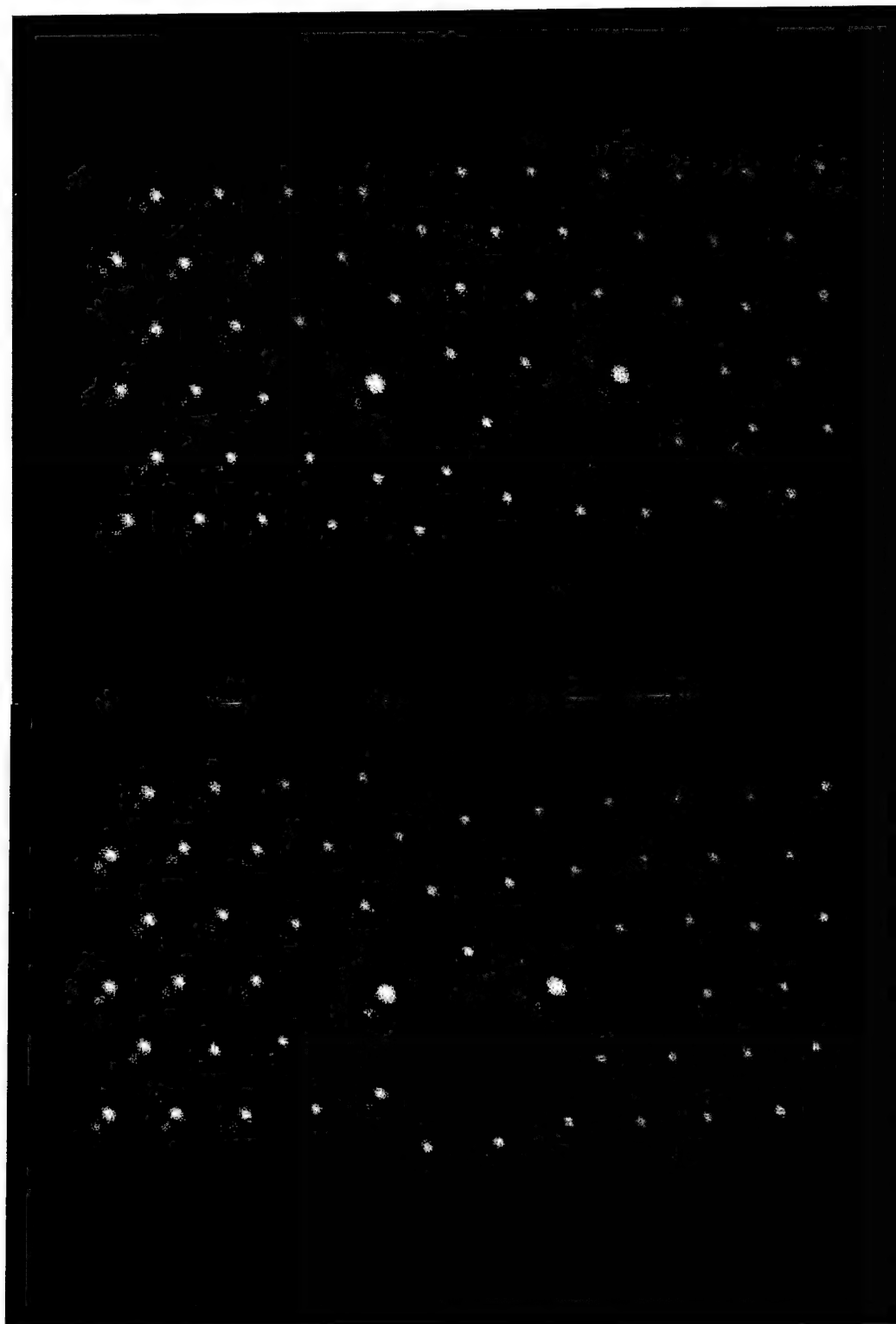
Figure 22
Two Snapshots from the Quantum Simulations of Two Atomic
Lithium Impurities in the Solid p-H$_2$ Lattice at 4 K

The top panel in Figure 22 is a configuration from the stable well region of Figure 20, while the lower panel is a configuration at the top of the barrier.

3.0 WORK IN PROGRESS

The quantum dynamical CMD method is presently being employed to computationally probe the explicit dynamical behavior of impurity species in solid para–hydrogen through very largescale computations. This effort is focused for the first time on the stability issue for cryogenic HEDM by explicitly studying the self-diffusion and recombination steps of the impurity atoms in the solid hydrogen host. The goal is to predict the maximum concentration of impurities that can be trapped as well as the effects of temperature, pressure, other impurities, etc. on the stability of the material. In the broadest context, the research effort addresses the critical "scale-up" issue for cryogenic HEDM.

4.0 RECOMMENDATIONS AND CONCLUSIONS FOR THE HEDM PROJECT

Given the encouraging results reported in this document and the outlook for future large-scale quantum dynamical simulations of low temperature HEDM systems, it is recommended that the Air Force should not abandon the low temperature solid hydrogen component of the HEDM Program. Scientists are only beginning to understand the nature of impurity trapping in these systems, and a wide range of different systems and experimental conditions remains to be explored. Computer modeling is poised to aid in the search for viable forms of low temperature HEDM.

5.0 REFERENCES

1. Fajardo, M. E., **Proceedings of the High Energy Density Matter Conference**, edited by M. E. Cordonnier, PL-CP-91-3003, OL-AC Phillips Laboratory, Edwards AFB, CA, Sep 1991.

2. Fajardo, M. E., "Matrix Isolation Spectroscopy of Metal Atoms Generated by Laser Ablation. II. The Li/Ne, Li/D_2, and Li/H_2 Systems," *J. Chem. Phys.*, **98**, 1993, pp. 110-118.

3. Smoluchowski, M., "Versuch einer mathematischen Theorie der Koagulationskinetik kolloider Lösungen," *Z. Phys. Chem.*, **92**, 1918, pp. 129-168.

4. Collins, F. C. and Kimball, G. E., "Diffusion-Controlled Reaction Rates," *J. Colloid Sci.*, **4**, 1949, pp. 425-437.

5. Noyes, R. M., *Prog. React. Kinet.*, **1**, 1961, pp. 129 (title not available).

6. Hynes, J. T., in **The Theory of Chemical Reaction Dynamics**, vol. IV, M. Baer, ed., CRC Press, Boca Raton, FL, 1985, p. 179, p. 210.

7. Eyring, H., "The Activated Complex in Chemical Reactions," *J. Chem. Phys.*, **3**, 1934, pp. 107-115.

8. Wigner, E., "Calculation of the Rate of Elementary Association Reactions," *J. Chem. Phys.*, **5**, 1937, pp. 720-725.

9. Miller, W. H., "Importance of Nonseparability in Quantum Mechanical Transition-State Theory," *Acc. Chem. Res.*, **9**, 1976, pp. 306-312.

10. Pechukas, P., "Transition State Theory," *Annu. Rev. Phys. Chem.*, **32**, 1981, pp. 159-177.

11. Truhlar, D. G., Hase, W. L., and Hynes, J. T., "Current Status of Transition-State Theory," *J. Phys. Chem.*, **87**, 1983, pp. 2664-2682.

12. Truhlar, D. G., and Garrett, B. C., "Variational Transition State Theory," *Annu. Rev. Phys. Chem.*, **35**, 1984, pp. 159-189.

13. Voth, G. A., "Feynman Path Integral Formulation of Quantum Mechanical Transition State Theory," *J. Phys. Chem.*, **97**, 1993, pp. 8365-8377.

14. Hänggi, P, Talkner, P., and Borkovec, M., "Reaction-Rate Theory: Fifty Years after Kramers," *Rev. Mod. Phys.*, **62**, 1990, pp. 250.

15. Silvera, I. F., "The Solid Molecular Hydrogens in the Condensed Phase: Fundamentals and Static Properties," *Rev. Mod. Phys.*, **52**, 1980, pp. 393-452.

16. Van Kranendonk, J., **Solid Hydrogen**, Plenum, New York, 1983.

17. Cao, J., and Voth, G. A., "A New Perspective on Quantum Time Correlation Functions," *J. Chem. Phys.*, **99**, 1993, pp. 10070-10073.

18. Cao, J., and Voth, G. A., "The Formulation of Quanatum Statistical Mechanics Based on the Feynman Path Centroid Density. II. Dynamical Properties," *J. Chem. Phys.*, **100**, 1994, pp. 5106-5117.

19. Cao, J., and Voth, G. A., "The Formulation of Quantum Statistical Mechanics Based on Feynman Path Centroid Density. III. Phase Space Formalism and Analysis of Centroid Molecular Dynamics," *J. Chem. Phys.*, **101**, 1994, pp. 6157-6167.

20. Cao, J., and Voth, G. A., "The Formulation of Quantum Statistical Mechanics Based on Feynman Path Centroid Density. IV. Algorithms for Centroid Molecular Dynamics," *J. Chem. Phys.*, **101**, 1994, pp. 6168-6183.

21. Calhoun, A., Pavese, M., and Voth, G. A., "Hyper-Parallel Algorithms for Centroid Molecular Dynamics: Application to Liquid *para*-Hydrogen," *Chem. Phys. Lett.*, **262**, 1996, 415-420.

22. Pavese, M., and Voth, G. A., "Pseudopotentials for Centroid Molecular Dynamics: Application to Self-Diffusion in Liquid para-Hydrogen," *Chem. Phys. Lett.*, **249**, 1996, pp. 231-236.

23. Li, D. H., and Voth, G. A., "A Path Integral Einstein Model for Characterizing the Equilibrium States of Low Temperature Solids," *J. Chem. Phys.*, **96**, 1992, pp. 5340-5353.

24. Li, D. H., and Voth, G. A., "A Variational Model for the Thermodynamical and Structural Properties of Impurities in Low Temperature Solids," *J. Chem. Phys.*, **98**, 1993, pp. 5734-5746.

25. Scharf, D., Martyna, G. J., Li, D. H., Voth, G. A., and Klein, M. L., "Nature of Lithium Trapping Sites in the Quantum Solids *para*-Hydrogen and *ortho*-Deuterium," *J. Chem. Phys.*, **99**, 1993, pp. 9013.

26. Li, D. H., and Voth, G. A., "Calculation of ESR Linewidths for Hydrogen Atom Impurities in Solid *para*-Hydrogen," *J. Chem. Phys.*, **100**, 1994, pp. 1785-1796.

27. Scharf, D., Martyna, G. J., and Klein, M. L., "Path-Integral Monte Carlo Study of a Lithium Impurity in *para*-Hydrogen: Clusters and the Bulk Liquid," *J. Chem. Phys.*, **99**, 1993, pp. 8997-9012.

28. Scharf, D., Martyna, G. J., and Klein, M. L., *Fizika Nizkikh Temperatur*, **19**, 1993, pp. 516-519 [Low Temp. Phys. **19**, 1993, 364] (title not available).

29. Scharf, D., Martyna, G. J., and Klein, M. L., "Path-Integral Monte Carlo Studies of *para*-Hydrogen Clusters," *J. Chem. Phys.*, **97**, 1992, pp. 3590-3599.

30. Scharf, D., Martyna, G. J., and Klein, M. L., "Isotope Effects on the Melting of para-Hydrogen and ortho-Deuterium Clusters," *Chem. Phys. Lett.*, **197**, 1992, pp. 231-235.

31. Feynman, R. P., **Statistical Mechanics**, Addison–Wesley, Reading, MA, 1972.

32. Feynman, R. P., and Hibbs, A. R., **Quantum Mechanics and Path Integrals,** McGraw-Hill, New York, 1965.

33. Berne, B. J., and Thirumalai, D., "On the Simulation of Quantum Systems: Path Integral Methods," *Annu. Rev. Phys. Chem.*, **37**, 1987, pp. 401-424.

34. Freeman, D. L., and Doll, J. D., "The Quantum Mechanics of Clusters," *Adv. Chem. Phys.*, **70B**, 1988, pp. 139-178.

35. Doll, J. D., and Freeman, D. L., *Adv. Chem. Phys.*, **73**, 1989, pp. 289 (title not available).

36. Doll, J. D., Freeman, D., and Beck, T. L., "Equilibrium and Dynamical Fourier Path Integral Methods," *Adv. Chem. Phys.*, **78**, 1990, pp. 61-127.

37. Doll, J. D., and Gubernatis, J. E., eds., **Quantum Simulations of Condensed Matter Phenomena,** World Scientific, Singapore, 1990.

38. Chandler, D., in **Liquides, Cristallisation et Transition Vitreuse, Les Houches, Session LI**, Levesque, D., Hansen, J. P., and Zinn-Justin, J. eds., Elsevier Science Publishers B.V., 1991.

39. Metropolis, N., Rosenbluth, A. W., Rosenbluth, M. N., Teller, A. H., and Teller, E., "Equation of State Calculations by Fast Computing Machines," *J. Chem. Phys.*, **21**, 1953 pp. 1087-1092.

40. Zoppi, M., and Neumann, M., "PIMC Simulations of Solid Parahydrogen," *Phys. Rev. B*, **43**, 1991, pp. 10242-10246.

41. Feynman, R. P., **Statistical Mechanics**, Addison–Wesley, Reading, MA, 1972, pp. 86-96.

42. R. P. Feynman, R. P., and Hibbs, A. R., **Quantum Mechanics and Path Integrals**, McGraw-Hill, New York, 1965, pp. 303-307.

43. Feynman, R. P., and Kleinert, H., "Effective Classical Partition Functions," *Phys. Rev. A*, **34**, 1986, pp. 5080-5084.

44. Giachetti, R., and Tognetti, V., "Variational Approach to Quantum Statistical Mechanics of Nonlinear Systems with Application to Sine-Gordon Chains," *Phys. Rev. Lett.*, **55**, 1985, pp. 912.

45. Giachetti, R., and Tognetti, V., "Quantum Corrections to the Thermodynamics of Nonlinear Systems," *Phys. Rev. B,* **33**, 1986, 7647-7658.

46. Cao, J., and Voth, G. A., "The Formulation of Quantum Statistical Mechanics Based on the Feynman Path Centroid Density. I. Equilibrium Properties," *J. Chem. Phys.,* **100**, 1994, pp. 5093-5105.

47. Liu, S., Horton, G. K., and Cowley, E. R., "Variational Path-Integral Theory of Thermal Properties of Solids," *Phys. Rev. B*, **44**, 1991, pp. 11714-11723.

48. Silvera, I. F., and Goldmam, V. V., "The Isotropic Intermolecular Potential for H_2 and D_2 in the Solid and Gas Phases," *J. Chem. Phys.*, **69**, 1978, pp. 4209-4213.

49. Rall, M., Zhou, D., Kisvarsanyi, E. G., and Sullivan, N. S., "Nuclear Spin-Spin Relaxation of Isotopic Impurities in Solid Hydrogen," *Phys. Rev. B* **45**, 1992, pp. 2800-2808.

50. Zhou, D., Edwards, C. M., and Sullivan, N. S., "Quantum Diffusion of Vacancies and Impurities in Solid Hydrogen," *Phys. Rev. Lett.*, **62**, 1989, pp. 1528-1531.

51. Collins, G. W., Souers, P. C., Maienschein, J. L., Mapoles, E. R., and Gaines, J. R., "Atomic-Hydrogen Concentrations in Solid D-T and T_2," *Phys. Rev. B* **45**, 1992, pp. 549-556.

52. Gaines, J. R., Tsugawa, R. T., and Souers, P. C., "An Estimate of the Thermal Conductivity of Solid T_2 from Pulsed NMR Data," *Phys. Lett. A* **84**, 1981, pp. 139-142.

53. Miyazaki, T., Iwata, N., Fueki, K., and Hase, H., "Observation of ESR Spin Flip Satellite Lines of Trapped Hydrogen Atoms in Solid H_2 at 4.2 K," *J. Phys. Chem.*, **94**, 1990, pp. 1702-1705.

54. Miyazaki, T., Iwata, N., Lee, K.-P., and Fueki, K., "Decay of H (D) Atoms in Solid Hydrogen at 4.2 K. Rate Constant for Tunneling Reaction H_2 (D_2, HD) + H(D)," *ibid.* **93**, 1989, pp. 3352-3355.

55. Danilowicz, R. L., and Etters, R. D., "Atomic-Hydrogen Impurities in Solid Molecular Hydrogen," *Phys. Rev. B* **19**, 1979, pp. 2321-2325.

56. Adrian, F. J., "Matrix Effects on the Electron Spin Resonance Spectra of Trapped Hydrogen Atoms," *J. Chem. Phys.* **32**, 1960, pp. 972-981.

57. Miyazaki, T., Morikita, H., Fueki, K., and Hiraku, T., "Trapping Sites of Hydrogen Atoms in Solid Hydrogen at 4.2 K Analyzed by ESR Linewidths," *Chem. Phys. Lett.*, **182**, 1991, pp. 35-38.

58. Tuckerman, M., Berne, B. J., Martyna, G. J., and Klein, M. L., "Efficient Molecular Dynamics and Hybrid Monte Carlo Algorithms for Path Integrals," *J. Chem. Phys,.* **99**, 1993, pp. 2796-2808.

59. Tuckerman, M., Marx, D., Klein, M. L., and Parrinello, M., "Efficient and General Algorithms for Path Integral Car-Parrinello Molecular Dynamics," *J. Chem. Phys.,* **104**, 1996, pp. 5579-5588.

60. Lobaugh, J., and Voth, G. A., "The Quantum Dynamics of an Excess Proton in Water," *J. Chem. Phys.*, **104**, 1996, pp. 2056-2069.

61. Calhoun, A., and Voth, G. A., "Electron Transfer Across the Electrode/Electrolyte Interface: Influence of Redox Ion Mobility and Counterions," *J. Phys. Chem.*, **100**, 1996, pp. 10746-10753.

6.0 LIST OF PUBLISHED ARTICLES FROM THE RESEARCH PROJECT

1. Pavese, M., and Voth, G. A., "Pseudopotentials for Centroid Molecular Dynamics: Application to Self-Diffusion in Liquid *para*-Hydrogen," *Chem. Phys. Lett.*, **249**, 1996, 231-236.

2. Li, D. H., and Voth, G. A., "Calculation of ESR Linewidths for Hydrogen Atom Impurities in Solid *para*-Hydrogen," *J. Chem. Phys.*, **100**, 1994, 1785-1796.

3. Li, D. H., and Voth, G. A., "A Variational Model for the Thermodynamical and Structural Properties of Impurities in Low Temperature Solids," *J. Chem. Phys.*, **98**, 1993, 5734-5746.

4. Scharf, D., Martyna, G. J., Li, D. H., Voth, G. A., and Klein, M. L., "Nature of Lithium Trapping Sites in the Quantum Solids *para*-Hydrogen and *ortho*-Deuterium," *J. Chem. Phys.*, **99**, 1993, 9013-9020.

5. Li, D. H., and Voth, G. A., "A Path Integral Einstein Model for Characterizing the Equilibrium States of Low Temperature Solids," *J. Chem. Phys.*, **96**, 1992, 5340-5343.

6. Scharf, D., Martyna, G. J., and Klein, M. L., "Path-Integral Monte Carlo Study of a Lithium Impurity in *para*-Hydrogen: Clusters and the Bulk Liquid," *J. Chem. Phys.*, **99**, 1993, 8997-9012.

7. Scharf, D., Martyna, G. J., and Klein, M. L., *Fizika Nizkikh Temperatur*, **19**, 1993, 516-519 [Low Temp. Phys. **19**, 1993, 364].

8. Scharf, D., Martyna, G. J., and Klein, M. L., "Path-Integral Monte Carlo Studies of *para*-Hydrogen Clusters," *J. Chem. Phys.*, **97**, 1992, 3590-3599.

9. Scharf, D., Martyna, G. J., and Klein, M. L., "Isotope Effects on the Melting of para-Hydrogen and ortho-Deuterium Clusters," *Chem. Phys. Lett.*, **197**, 231-235.

7.0 LIST OF INVITED LECTURES ON RESULTS FROM THE RESEARCH PROJECT

1. "A Quantum Mechanical Perspective on Activated Rate Processes," Physical Chemistry Seminar, University of Illinois at Urbana-Champaign, February, 1991.

2. "Activated Dynamics: A Unified Classical and Quantum Perspective," Packard Fellowship Holders Annual Meeting, Monterey, California, September, 1991.

3. Invited Participant in the National Academy of Sciences "National Symposium on Frontiers of Science," Irvine, California, November, 1991.

4. "Recent Advances in the Quantum Theory of Chemical Reaction Rates," Physical Chemistry Seminar, Boston University, February, 1992.

5. "Recent Advances in the Quantum Theory of Chemical Reaction Rates," Physical Chemistry Seminar, University of Wisconsin, February, 1992.

6. "Effect of Nonlinearity on Tunneling in Condensed Matter Systems," Symposium on Tunneling in Condensed Matter Systems, March Meeting of the American Physical Society, March, 1992.

7. "Quantum Path Integral Simulations of Impurity Atoms in Solid Hydrogen," Workshop on the Properties of Solid Hydrogen, Honolulu, HI, March, 1992.

8. "Quantum Path Integral Simulations of Impurity Atoms in Solid Hydrogen," Air Force High Energy Density Materials Contractors Meeting, Lancaster, CA, April, 1992.

9. "Recent Advances in the Quantum Theory of Chemical Reactions," Physical Chemistry Seminar, University of Texas at Austin, April, 1992.

10. "Recent Advances in the Theory of Condensed Phase Chemical Reactions," Chemistry Department Seminar, University of Pittsburgh, October, 1992.

11. "Recent Advances in the Theory of Condensed Phase Chemical Reactions," Physical Chemistry Seminar, Northwestern University, November, 1992.

12. "Recent Advances in the Theory of Condensed Phase Chemical Reactions," Physical Chemistry Seminar, Argonne National Laboratory, November, 1992.

13. "Recent Advances in the Theory of Condensed Phase Chemical Reactions," Chemistry Department Seminar, Cornell University, December, 1992.

14. "Recent Advances in the Theory of Condensed Phase Chemical Reactions," Physical Chemistry Seminar, Brown University, December, 1992.

15. "The Theory of Chemical Reactions in Condensed Phases: Quantum and Classical Perspectives," Chemistry Department Seminar, Columbia University, March, 1993.

16. "The Theory of Chemical Reactions in Condensed Phases: Quantum and Classical Perspectives," Physical Chemistry Seminar, The Ohio State University, April, 1993.

17. "Quantum Mechanical Calculations of Tunneling Rates in Condensed Phase Systems," The 26th Jerusalem Symposium on Quantum Chemistry and Biochemistry, Jerusalem, Israel, May 1993.

18. "Quantum Mechanical Studies of Tunneling Processes in Many-Body Systems," Eighth American Conference on Theoretical Chemistry, Rochester, NY, June 1993.

19. "The Quantum Theory of Condensed Phase Chemical Reactions," Physical Chemistry Seminar, University of California, San Diego, September, 1993.

20. "The Quantum Theory of Condensed Phase Chemical Reactions," Physical Chemistry Seminar, University of Maryland, September, 1993.

21. "The Quantum Theory of Condensed Phase Chemical Reactions," Physical Chemistry Seminar, Massachusetts Institute of Technology, October, 1993.

22. "A New Perspective on Quantum Dynamics in Condensed Matter Systems," Physics Colloquium, Drexel University, March, 1994.

23. "A New Perspective on Quantum Dynamics in Condensed Matter Systems," Telluride Workshop on Dynamics in Condensed Matter, Telluride, Colorado, July, 1994.

24. "The Computation of Quantum Mechanical Time Correlation Functions," Symposium on Coherence in Condensed Phase Chemical Dynamics, Fall Meeting of the American Chemical Society, Washington, D.C., August 1994.

25. "Quantum Computer Simulations of Impurities in Low Temperature Solids," Joint Meeting of the Department of Defense and National Consortium of High Performance Computing Computational Chemistry and Materials Science Group, Pittsburgh Supercomputing Center, Carnegie-Mellon University, August, 1994.

26. "Classical and Quantum Aspects of Activated Dynamics," CECAM Workshop on Barrier Crossing Dynamics, Lyon, France, October, 1994.

27. "A Computational Approach to Quantum Dynamics in Low Temperature Solids," Conference on The Physics and Chemistry of Quantum Solids, Fluids, Films, and Clusters, Newport Beach, CA, February, 1995.

28. "The Computation of Quantum Mechanical Time Correlation Functions: A Dynamical Role for the Feynman Path Centroid Variable?", Workshop on Effective Potential Methods for Quantum Effects in Condensed Matter, Florence, Italy, February, 1995.

29. "A New Perspective on Quantum Dynamics: Building on Feynman's Legacy," Seminar at the Laboratory of the Theoretical Physics of Liquids, Université Pierre et Marie Curie, Paris, France, March, 1995.

30. "Feynman Path Centroid Methods for Condensed Phase Quantum Dynamics," Invited Lecturer at the Summer School on Monte Carlo and Molecular Dynamics in Condensed Matter Systems, Como, Italy, July, 1995.

31. "Quantum Simulations of Proton Motion in Condensed Media," Symposium on Proton Transfer, Fall Meeting of the American Chemical Society, Chicago, IL, August, 1995.

32. "Some New Perspectives and Results on Quantum Dynamics in Condensed Phases," Physical Chemistry Seminar, Colorado State University, September, 1995.

33. "The Theoretical Description of Complex Condensed Phase Dynamics with Applications to Solution Phase Chemistry, Biophysics, and Electrochemistry," Chemical Physics Colloquium, University of Colorado, September, 1995.

34. "Quantum Dynamics in Condensed Phases: Some New Theoretical Methods with Applications to Acid-Base Chemistry, Biophysics, and Electrochemistry," Physical Chemistry Seminar, University of Utah, October, 1995.

35. "The Quantum Theory of Condensed Phase Dynamics with Applications to Solution Phase Chemistry, Biophysics, and Electrochemistry," Physical Chemistry Seminar, University of Minnesota, October, 1995.

36. "New Approaches for the Simulation Of Condensed Phase Quantum Dynamics," Invited Lecture, 36th Annual Sanibel Symposium, St. Augustine, FL, February, 1996.

37. "The Simulation of Quantum Dynamical Phenomena in Condensed Matter," Invited Lecture, International Congress on Theoretical Chemical Physics, New Orleans, LA, March, 1996.

38. "New Approaches for the Simulation Of Condensed Phase Quantum Dynamics," Invited Seminar, National Institute of Standards and Technology, Gaithersburg, MD, May, 1996.

39. "New Theoretical Approaches for Condensed Phase and Biophysical Dynamics," Invited Seminar, Telluride Summer Research Workshop on Structure and Dynamics of Biophysical and Condensed Matter Systems, Telluride, Colorado, July, 1996.

40. "Parallel Simulation of Quantum Dynamical Phenomena in Condensed Matter," Invited Seminar, Department of Defense High Performance Computing Software Initiative Meeting, Ames, Iowa, September, 1996.

8.0 CONTRIBUTION OF THE PROJECT TO THE TRAINING OF MANPOWER IN THE HEDM FIELD

This research project supported four postdoctoral fellows over five years. Two have taken jobs in academics (Indiana University and University of California, San Diego) and two in biomedical research. The former have continued an interest in HEDM research.